Production of light particles in nucleus–nucleus collisions (experimental facts, theoretical models, possible experiments)

V. I. Zagrebaev
Chuvash State University, Cheboksary

Yu. É. Penionzhkevich
Joint Institute for Nuclear Research, Dubna

Fiz. Elem. Chastits At. Yadra **24**, 295–347 (March–April 1993)

The basic experimental results on the yield of light particles in nucleus–nucleus collisions at low and medium energies are reviewed. An analysis is made of the inclusive spectra of light particles and also their yield in coincidence with characteristic x rays, γ rays, projectilelike fragments, other light particles, fission fragments, and recoil nuclei. The main theoretical models used to describe the yield of light particles, their achievements, and shortcomings are briefly described. The currently unresoived problems in the production of light particles, in particular, and of the dynamics of two-nucleus interaction, in general, and also possible experiments capable of clarifying the situation in this field are discussed.

INTRODUCTION

The problem of the production of light particles (with mass less than the mass of any of the colliding nuclei) is a most intriguing problem in heavy-ion physics. Hundreds of experimental and theoretical studies have been devoted to this problem. A strong yield of fast α particles in reactions with complex nuclei was already observed in 1961.[1] However, strong interest in this problem arose only at the end of the seventies (and it continues to the present day), after numerous experimental groups had begun to make more systematic inclusive and correlation measurements of processes involving the production of light particles. In this connection, we should mention the most complete results obtained at the Hahn–Meitner Institute (Berlin),[2–8] Groningen (Holland),[9–16] the Laboratory of Nuclear Reactions at the Joint Institute for Nuclear Research,[17–23] and at the University of Michigan in the United States (Refs. 26, 61, 66, 67, and 78). In our view, there are several reasons for the great interest in the problem of the production of light particles in heavy-ion collisions. First, the cross section for the production of light particles is extremely large (comparable with the total reaction cross section), and, therefore, the production of light particles is a characteristic feature of nucleus–nucleus collisions, the complete understanding of which is impossible without an understanding of the mechanism of production of these particles. Second, as experimental investigations showed, the properties of the energy, mass, and angular distributions of the emitted particles were to a large degree unexpected, and sometimes also difficult to explain. Finally, it was firmly established that a significant (sometimes the largest) proportion of these particles is emitted in the initial stage of interaction of the two nuclei and, therefore, carries direct information about the dynamics of this interaction, in contrast to the products of the decay of a compound system, which has effectively "forgotten" the entire history of its formation.

In this review, we have concentrated our attention primarily on the physically most transparent and comprehensible experimental facts, confirmed in several studies, attempting to explain what we already know fairly reliably and what we do not yet know about the mechanisms of production of the light particles and the dynamics of two-nucleus interactions. The desired aim of this analysis is, above all, the planning of new experiments; we also wish to stimulate the development of new theoretical approaches.

Since the most complete experimental data on the production of light particles have been obtained at low and medium energies, the main attention in this review will be devoted to energies up to 100 MeV/nucleon.

1. WHAT WE KNOW ABOUT THE PRODUCTION OF LIGHT PARTICLES (EXPERIMENTAL FACTS)

1.1. Inclusive spectra

Mass distribution of light particles

At low energies, α particles and protons are predominantly produced in nucleus–nucleus collisions (Fig. 1), α particles being predominant at forward angles (Fig. 2). As the energy of the incident ion is increased, the yield of all light particles increases, but at an energy above 100 MeV/nucleon the nature of the mass distribution changes abruptly—the yield of light particles decreases monotonically with increasing mass of the particles (Fig. 3). This can be interpreted as predominance of a gaseous phase in the region of overlap of the two nuclei at these energies.

Energy distribution

The main feature of the energy spectra of the light particles is that for forward and even for lateral angles these spectra are much harder than evaporation spectra (Fig. 4). For clarity, Fig. 5 shows the velocity distributions of the α particles. These are actually the same energy spectra, represented as functions of the α-particle velocity at the barrier:

$$\frac{v_\alpha(B)}{v_{\text{beam}}(B)}=\left(\frac{m_I}{m_\alpha}\frac{E_\alpha-V_c^B(\alpha)}{E_I-V_c^B(I)}\right)^{1/2}.$$

 1063-7796/93/020125-24$10.00

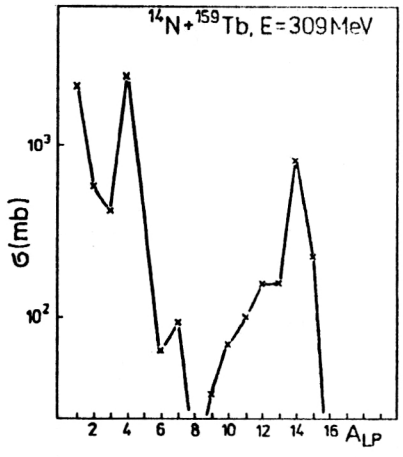

FIG. 1. Integrated (over the angles) cross section for the production of light products in the $^{14}N+^{159}Tb$ reaction at $E_N=309$ MeV (for $A=14$ without elastic scattering of ^{14}N).[13]

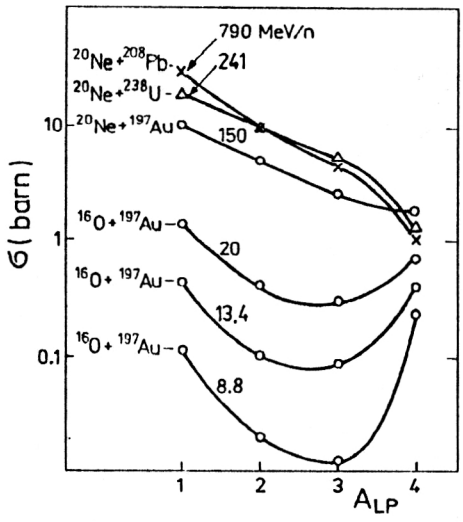

FIG. 3. Cross sections for production of light particles as functions of the energy of the incident ion (the numbers next to the curves stand for MeV/nucleon).[25]

Finally, Fig. 6 shows energy spectra of α particles obtained at the Laboratory of Nuclear Reactions at the JINR, where a special study was made of the high-energy part of these spectra. The main properties of the inclusive energy spectra of the light particles are as follows:

1) The maximum of the spectrum is always situated at a velocity of the light particle less than the beam velocity: $v_{LP}^{OPT}<v_{beam}$, and this indicates that relaxation processes play an important part in the stage at which light particles are emitted.

2) With increasing beam energy E_I, the peak of the double differential cross section for the yield of light particles is displaced toward the energy corresponding to the beam velocity ($v_{LP}^{OPT}\to v_{beam}$), but even at an energy of several tens of mega-electron-volts per nucleon the spectrum of light particles emitted forward contains an appreciable "dissipative" part ($V_c^B(\alpha)<E_\alpha<E_\alpha^{beam}$).

3) The lower the projectile mass A_I, the closer the peak approaches to v_{beam} (the smaller the "dissipative" part of the spectrum).

4) With increasing energy of the incident ion, the maximum of the differential cross section $d^2\sigma/d\Omega dE(v_{LP}^{OPT})$ initially rapidly increases (by an order of magnitude on the transition from $E_I=5$ MeV/nucleon to $E_I=20$ MeV/nucleon), but one then observes a certain saturation (Fig. 5).

5) At not too high energies ($E_I=8$ MeV/nucleon) the energy spectrum of the light particles extends up to the two-body kinematic limit [corresponding to fusion of the projectile remnant (*I–LP*) and the target with production of a final nucleus in the ground state], an abrupt break being observed at the very end of this spectrum (Fig. 6).

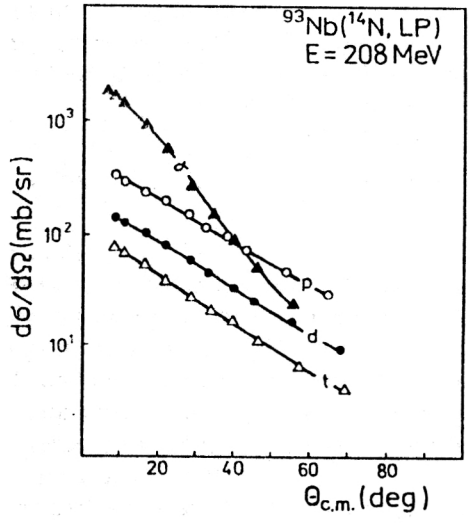

FIG. 2. Integrated (over the energy) angular distributions of light particles in the $^{93}Nb(^{14}N,LP)$ reaction at $E_{lab}=208$ MeV.[24]

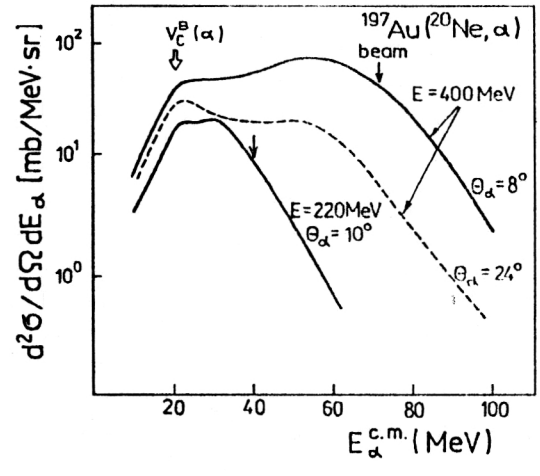

FIG. 4. Energy spectra of α particles produced in the $^{197}Au(^{20}Ne,\alpha)$ reaction.[3] The arrows show the energies of the α particles corresponding to the beam velocity and to the height of the Coulomb barrier in the exit channel.

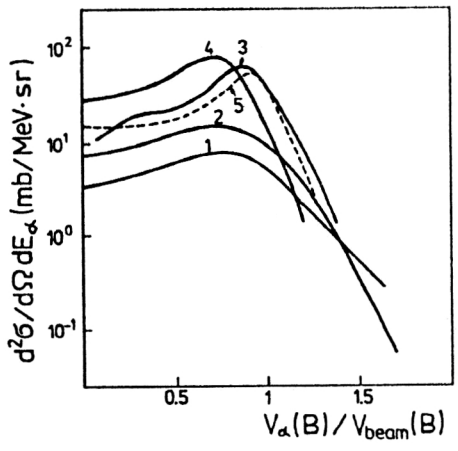

FIG. 5. Distribution of α particles with respect to the velocities in the following reactions: *1)* ^{181}Ta(^{22}Ne,α) (E_f=6.4 MeV/nucleon, ϑ_α=20°) (Ref. 20); *2)* ^{181}Ta(^{22}Ne,α) (8.1 MeV/nucleon, 20°) (Ref. 20); *3)* ^{93}Nb(^{14}N,α) (15 MeV/nucleon, 7°) (Ref. 24); *4)* ^{197}Au(^{20}Ne,α) (20 MeV/nucleon, 8°) (Ref. 3); *5)* ^{197}Au(^{14}N,α) (35 MeV/nucleon), 9.5°) (Ref. 26).

Angular distributions of light particles

At above-barrier energies of the incident ion, the light particles produced in the reaction have a general forward directionality, this being greater, the higher their energy (Fig. 7a). In the inclusive angular distributions of the light particles there is actually no manifestation of the angle of a grazing collision, which is clearly observed in the distributions of heavy fragments. This may indicate that a broader range of impact parameters of the projectile contributes to the production of the light particles. The decrease of the experimental cross section by several orders of magnitude on the transition from forward to lateral angles in the angular distribution of the light particles with velocities close to the beam velocity (i.e., at the maximum of the energy spectrum) is indisputable evidence of a nonequilibrium mechanism of their production in the initial stage of the reaction before complete relaxation of the kinetic energy.

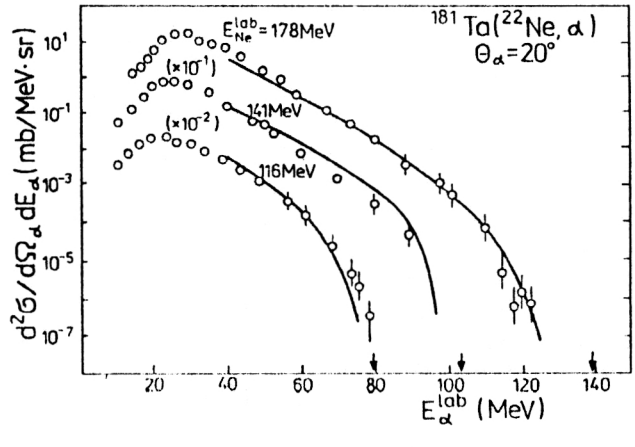

FIG. 6. Energy spectra of α particles in the ^{181}Ta(^{22}Ne,α) reaction measured at ϑ_α=20° for three different beam energies: 116, 141, and 178 MeV. The continuous curves represent the theoretical calculation in the model of dissipative mass transfer.

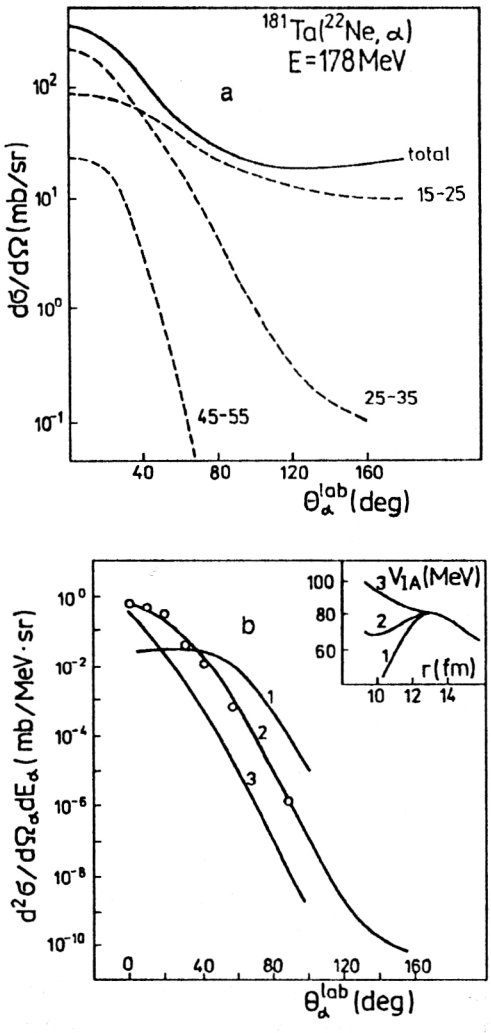

FIG. 7. a—Angular distributions of α particles in different energy intervals (numbers in mega-electron-volts next to the curves) produced in the ^{181}Ta(^{22}Ne,α) reaction at E_{lab}=178 MeV.[20] The beam velocities correspond to the energy E_α=30 MeV. b—Sensitivity of the angular distribution of the light particles to the form of the internuclear interaction in the region beyond the Coulomb barrier in the model of dissipative mass transfer.[99]

We could obtain much more information from the angular distributions of the light particles if they could be measured not only in distinguished energy windows but also in fairly narrow windows of the angular-momentum transfer to the final nucleus.

Yield of light particles as a function of the projectile energy

Unfortunately, there have not been enough systematic measurements of the yield of light particles in a wide range of initial energies for a given pair of colliding nuclei. Figure 8 shows the integrated (over the angles) total cross sections for production of α particles in the ^{159}Tb(^{14}N,α) reaction as a function of the energy of the incident ion.[15] The sharp increase in the yield of α particles with increasing initial energy in the region $E_N \leqslant 10$ MeV/nucleon is undoubtedly due to transition to the above-barrier region, i.e., the overcoming of the Coulomb screening of the total geometrical cross section of the colliding nuclei. The fur-

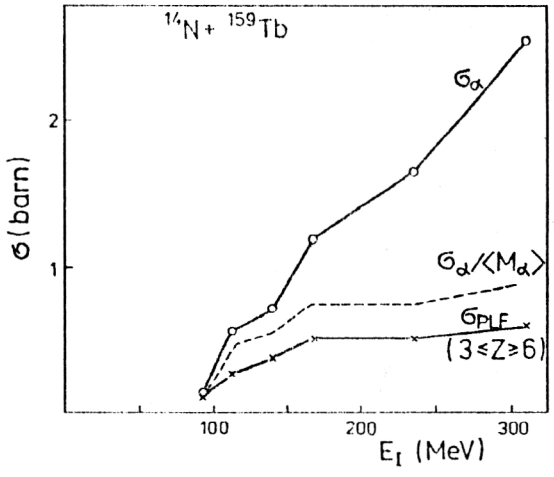

FIG. 8. Integrated (over the angles) cross section for production of α particles and projectilelike fragments with $3 \leqslant Z \leqslant 6$ in the $^{14}N + ^{159}Tb$ reaction as a function of the beam energy.[15]

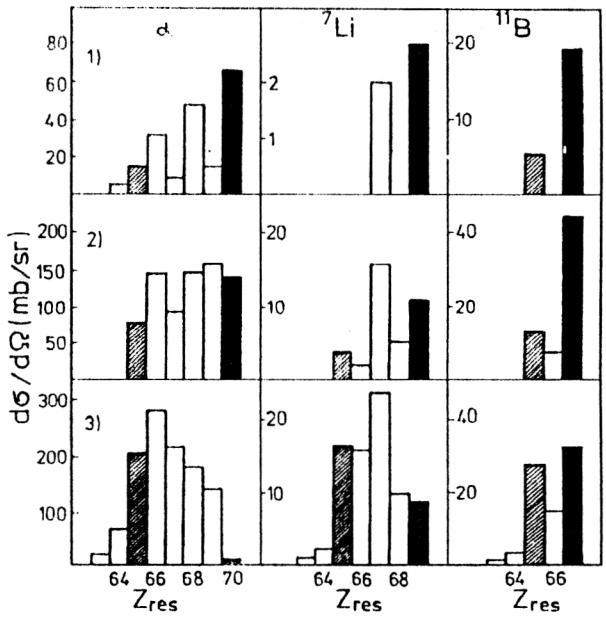

FIG. 9. Partial differential cross sections for production of light fragments (in coincidence with fixed charge of the final nucleus) in the $^{14}N + ^{159}Tb$ reaction for different initial energies: 1) 115 MeV, $\vartheta_{PLF} = 30°$; 2) 165 MeV, 20°; 3) 236 MeV, 20°.[14] The black rectangles correspond to the lower limit of the binary process ($\Delta Z = 0$, i.e., $Z_{res} = Z_A + Z_{proj} - Z_{LP}$), and the hatched rectangles to $Z_{res} = Z_A$.

ther increase in the yield of α particles with increasing E_N is due to the increase in their multiplicity, which grows with E_N in proportion to the cross section σ_α itself.[15]

1.2. Coincidences with characteristic radiation of the final nuclei (Refs. 12–16, 21, and 28)

At first glance, one might suppose that in experiments to detect light particles in coincidence with characteristic KX radiation the different reaction channels could be directly distinguished and, thereby, the mechanism of production of the light particles established. However, this cannot be done at fairly high energies, since the deexcitation time of the KX radiation greatly exceeds the characteristic nuclear time (including, evidently, the lifetime of the compound nucleus), and this prevents us from "discerning" the primary process. Nevertheless, the KX method can give a large amount of useful information, especially at low energies, when the excitation energy of the reaction products is not very high.

Let us consider a collision of a projectile I with a target A, with detection of a light fragment PLF and characteristic KX radiation (i.e., the charge) of the heavy residual nucleus B:

$$I + A \rightarrow \text{primary process} \rightarrow \text{PLF} + B + X.$$

In this experiment, we know the charge $\Delta Z = Z_I + Z_A - Z_{PLF} - Z_B$ that is carried away by one or several particles X, which can be produced either by fragmentation of the projectile (or decay of an excited primary fragment PLF^*_{pr}) or as a result of evaporation from a primary excited heavy nucleus B^*_{pr}. Note that the cross section in the channel with $\Delta Z = 0$, for example, corresponds only to a lower limit of the primary binary process, while the sum of channels with $Z_B \leqslant Z_A$, conversely, corresponds to an upper bound of the elastic and inelastic processes of fragmentation of the incident ion. Figure 9 shows the partial cross sections for the yield of different light fragments produced in the $^{14}N + ^{159}Tb$ reaction and accompanied by a final nucleus with charge Z_B.[14,15]

Thus, we see that at the given energies the main contribution to the production of light particles is made by channels with charge transfer ($Z_B > Z_A$). In contrast, at low energies the dominant process is the binary mechanism of mass transfer (or incomplete fusion), i.e., $Z_B = Z_A + Z_I - Z_{PLF}$. The fact that the α particles produced in the binary process are not evaporation products was convincingly demonstrated in Ref. 21, in which a careful measurement was made of the energy spectrum of α particles in coincidence with KX radiation corresponding to $Z_B = Z_A + Z_I - Z_\alpha$ in the $^{22}Ne + Ta \rightarrow \alpha + Tl + xn$ reaction at $E_{Ne} = 155$ MeV. The spectrum was shown to be much harder than an evaporation spectrum and close to the inclusive spectrum of the α particles. A second conclusion which can be drawn from Fig. 9 is that the processes of breakup (fragmentation) of the incident ion that are not accompanied by charge transfer (i.e., $Z_B \leqslant Z_A$) do not make a very large contribution to the yield of light particles at energies $E \leqslant 20$ MeV/nucleon and angles $\vartheta_\alpha \geqslant 20°$. Numerous other rather interesting conclusions were drawn in Refs. 12–16 concerning the light-particle production mechanism, but we shall not give them here, since they were based on additional (admittedly entirely reasonable) assumptions concerning the decay of excited primary products and the nature of the "lost" charge ΔZ.

1.3. Coincidences with neutrons (Refs. 4–6 and 27)

The number of evaporated neutrons is uniquely related to the excitation energy of the final nucleus. Therefore, α

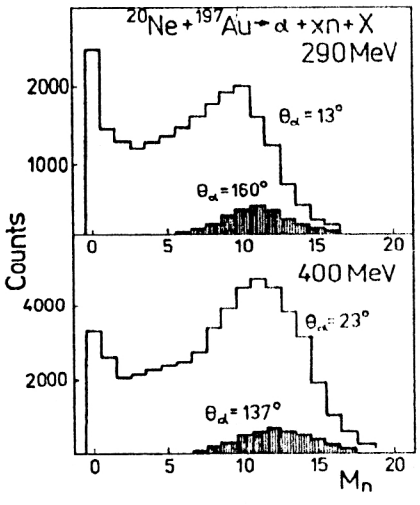

FIG. 10. Distribution of the multiplicity of neutrons accompanying an α particle in the $^{20}Ne+^{197}Au \rightarrow xn+X$ reaction.[5]

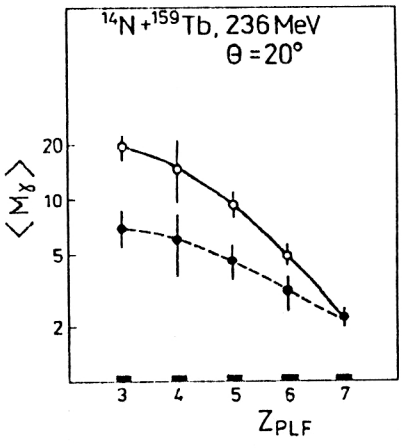

FIG. 12. Mean γ multiplicity in the $^{14}N+^{159}Tb$ reaction at $E=236$ MeV and $\vartheta_{PLF}=20°$ as a function of the charge of the detected fragment. The upper curve corresponds to the binary process $\Delta Z=(Z_A+Z_I)-(Z_B+Z_{PLF})=0$ (see Sec. 1.2), and the lower curve to the channel with fixed charge $Z_B=Z_A=65$ of the final nucleus.

particles accompanied by a low neutron multiplicity M_n are produced in peripheral processes of projectile breakup (direct or sequential) with small energy and mass transfer to the target nucleus. In contrast, α particles accompanied by a large number of neutrons are produced in processes with larger overlap of the colliding nuclei. Figure 10 shows the distribution measured in the $^{20}Ne+^{197}Au$ reaction of the multiplicity of neutrons emitted together with an α particle.[5]

Using these data, we can distinguish three components in the inclusive yield of α particles (Fig. 11):

1) the isotropic ("evaporation") part, which does not exceed a few percent for the forward angles;

2) "breakup" α particles;

3) "nonequilibrium" forward-directed α particles accompanied by a large number of neutrons.

The fraction of "breakup" α particles does not exceed 40% of all the "nonevaporation" α particles at energies $E_{Ne} \leqslant 20$ MeV/nucleon.[5] The energy spectrum of the "breakup" α particles is broader than the spectrum of the "nonequilibrium" α particles.[5] Unfortunately, the experimental possibilities did not permit measurement of these spectra in a sufficiently wide range, in particular, in their most interesting hard part.

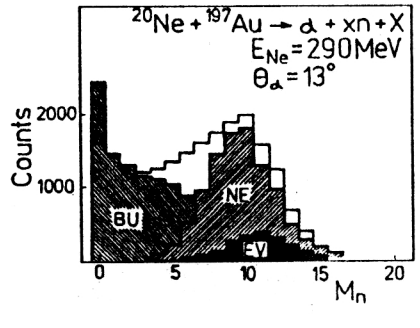

FIG. 11. Separation of neutron multiplicity in the channel with emission of an α particle into three components: EV, neutrons accompanied by evaporated α particles (obtained from the count at backward angles); NE, neutrons accompanying "nonequilibrium" α particles (symmetric Gaussian in the region of the central peak, obtained after subtraction of the evaporation part); BU, the "breakup" component in the yield of α particles (the remaining part at small M_n).[5]

1.4. Coincidences with γ rays (Refs. 10, 14, 21, and 28–43)

The main aim in the measurement of the multiplicity of γ rays accompanying the emission of a light particle is to establish the angular-momentum transfer to the nucleus and thus establish which collisions (central or peripheral) of the initial nuclei predominantly produce the light particles.

Figure 12 shows the mean γ multiplicity as a function of the charge of a light fragment emitted at angle 20° in the $^{14}N+^{159}Tb$ reaction at $E_N=236$ MeV.[14] The simultaneous detection of the KX radiation made it possible to determine the charge of the final nucleus as well. The increase of the mean γ multiplicity with increasing mass of the fragment transferred from the projectile to the target (I–PLF)—the upper curve in Fig. 12—unambiguously indicates a *quasi-direct* (fast, few-step) and *peripheral* nature of such transfer—the angular-momentum transfer λ_{tr} is proportional to the mass transfer $\Delta m_{tr}=m_I-m_{PLF}$. It is much harder to interpret the lower curve in the same figure, which corresponds to $Z_B=Z_A$. The channel with $Z_B=Z_A$ is due both to the process of breakup of the incident ion (in this case, the conjugate products $Z_{PLF}=3$ and 4, $Z_{PLF}=5$ and 2 should have the same values of M_γ) and to transfer processes with production of a highly excited primary nucleus B^*_{pr}, which evaporates charged particles and goes over into the final nucleus B that is detected by means of the KX radiation. Although both processes are obviously peripheral, the angular-momentum transfer in them is much less than in the peripheral process of mass transfer. Table I gives data on the mean γ multiplicity in the $^{124}Sn(^{16}O, \alpha Xn)$ reaction at $E_{lab}=90$ and 100 MeV.[42] The

TABLE I. Mean γ multiplicity measured in coincidence with fast α particles emitted at angle $13.5 < \vartheta_\alpha < 37$ in the $^{16}O + ^{124}Sn$ reaction.[42]

Energy, MeV	Reaction channel	M_γ	σ_{M_γ}	$<L_i>$
90	$(\alpha, 3n)$	13.4	7,3	32,4
	$(\alpha, 4n)$	12,7	5,5	29,4
100	$(\alpha, 4n)$	15,7	6,8	38,5
	$(\alpha, 5n)$	12,6	7,5	32,7

mean value of the angular momentum $\langle L_i \rangle$ in the entrance channel corresponding to this reaction was determined from M_γ with allowance for the angular momentum carried away by the α particle for beam velocity $\approx \langle L_i \rangle m_\alpha / m_I$ and by evaporated neutrons.

Two main conclusions can be drawn from the analysis of these data.

1) The mean value of the impact parameter $\langle b_i \rangle = \langle L_i \rangle / k_i$ in the channel with light-particle emission corresponds to peripheral but not limiting grazing collisions: $\langle b_i \rangle = 4.2$ fm $< b_{gr} \approx 6$ fm at $E = 90$ MeV.

2) The width of the γ multiplicity and, therefore, the width of the L window of the channel with emission of fast light particles is very broad: $\sigma_{M_\gamma}/M_\gamma \approx 0.5$ (this, incidentally, is not surprising if one bears in mind the large cross section for production of light particles).

Figure 13 shows the mean γ multiplicity and the mean angular-momentum transfer $\langle \lambda_{tr} \rangle$ to the final nucleus deduced from it as functions of the energy of α particles emitted forward in the $Ta(^{22}Ne,\alpha)$ reaction at $E_{Ne}^{lab} = 155$ MeV.[20] Calculation of the angular-momentum transfer λ_{tr} in the entrance L_i (with allowance for the increase with increasing E_α in the angular momentum carried away by the α particle) shows that the mean value of the angular momentum $\langle L_i \rangle$ in the entrance channel depends rather weakly on the energy of the α particle emitted forward, remaining at the level $\approx 50\hbar$, this being somewhat less than $L_{grazing}$ for this reaction.

1.5. Coincidences with projectilelike fragments (Refs. 2, 7, 9, 11, and 44–63)

Experiments on coincidences of light particles with a residual fragment permit direct conclusions to be drawn about the role of the process of breakup (fragmentation) of the incident ion in the formation of the fast light particles and about the breakup mechanism itself (elastic, inelastic, direct, sequential?). However, the interpretation of such experiments is extremely complicated, since the results depend very strongly on the emission angles of the detected fragments, and different breakup mechanisms (for example, direct and sequential) have essentially the same characteristic properties. In addition, without the use of 4π detectors it is very difficult to integrate over all angles (in the reaction plane and out of it) of the light particle associated with the fragment in order to deduce the absolute value of the breakup cross section and its fraction in the inclusive yield of light particles as a function of their energy and emission angle.

Figure 14 shows the relative yield of projectilelike fragments in coincidence with an α particle in the $^{20}Ne + ^{93}Nb \to \alpha + PLF + X$ reaction at $E_{Ne} = 30$ MeV/nucleon. Figure 15, which is based on kinematic consider-

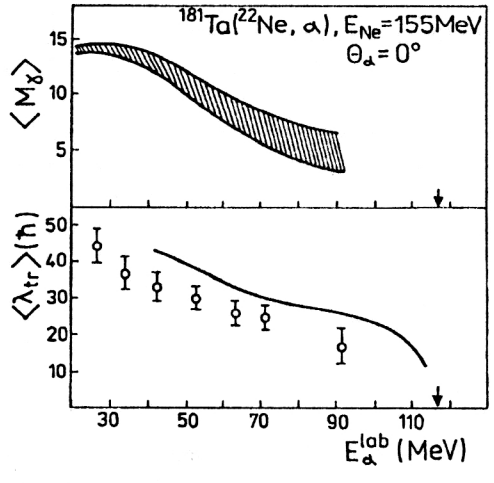

FIG. 13. Mean γ multiplicity and angular-momentum transfer in the reaction as functions of the energy of α particles emitted at small angles.[21] The theoretical curve is for the model of the dissipative incomplete-fusion reaction.[99]

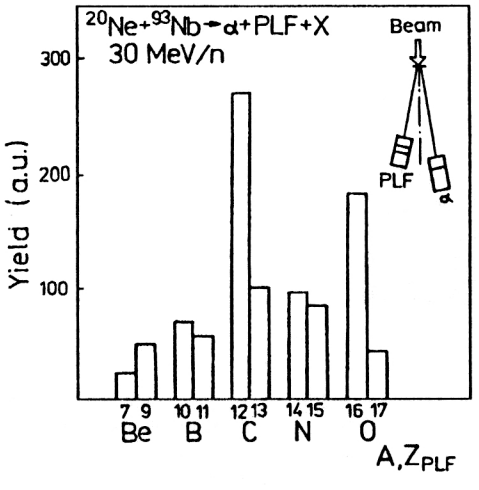

FIG. 14. Yield of light fragments in coincidence with an α particle in the $^{20}Ne + ^{93}Nb \to \alpha(8.5°) + PLF(-8.5°) + X$ reaction at beam energy 30 MeV/nucleon.[60]

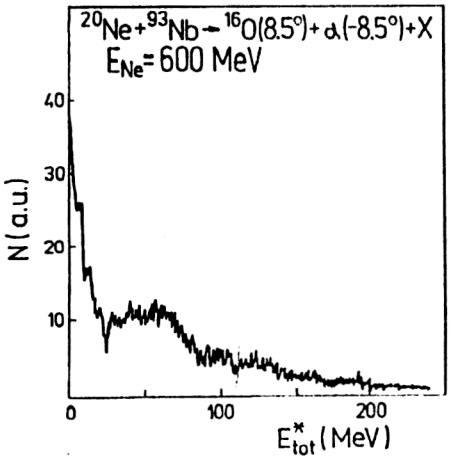

FIG. 15. Spectrum of total excitation energy in the $^{20}Ne+^{93}Nb\rightarrow{}^{16}O(-8.5°)+\alpha(8.5°)+X$ reaction at energy $E_{Ne}=600$ MeV under the assumption of three-body kinematics of the process.[60]

ations, shows the spectrum of the total excitation of the target and projectile in the purely breakup channel $^{20}Ne+^{93}Nb\rightarrow{}^{16}O+\alpha+X$, while Fig. 16 shows the analogous spectrum for the exit channel $^{12}C+\alpha$ in the same reaction; this can be interpreted as breakup of an excited $^{16}O^*$ nucleus obtained as a result of transfer of an α particle. The total excitation energy E^*_{tot}, i.e., the energy dissipated in the entrance channel, is determined under the assumption of three-body kinematics:[60]

$$E^*_{tot}=E^*_{PPLF}+E^*_{TLF}$$
$$=[E^{LP,PLF}_{rel}-Q_{PPLF}]$$
$$+[E_{proj}-(E_{PLF}+E_{LP}+E_{TLF})+Q_{ggg}],$$

where $E^{LP,PLF}_{rel}$ is the energy of the relative motion of the light particle and the detected fragment, $Q_{PLF}=m_{PPLF}-m_{LP}-m_{PLF}$, PPLF=LP+PLF, $Q_3=-[E_{proj}-(E_{PLF}+E_{LP}+E_{TLF})]$, $Q_{ggg}=(m_p+m_T)-(m_{LP}+m_{PLF}+m_{TLF})$. Finally, Fig. 17 shows the Q_3 spectrum, which characterizes the inelasticity of the $^{16}O+^{197}Au\rightarrow\alpha+^{12}C+X$ reaction at $E_{^{16}O}$ = 424 and 520 MeV.[59]

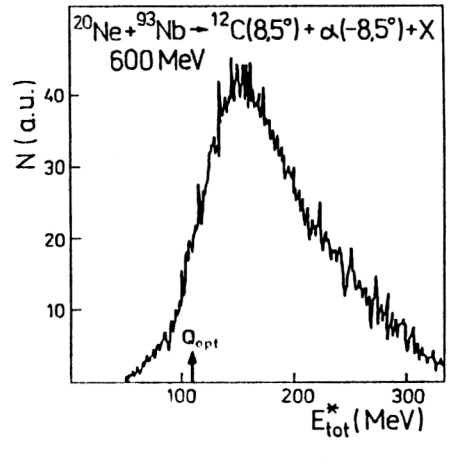

FIG. 16. Spectrum of energy dissipated in the entrance channel in the $^{20}Ne+^{93}Nb\rightarrow{}^{12}C(8.5°)+\alpha(-8.5°)+X$ reaction at $E_{Ne}=600$ MeV.[60]

Although the detected particles (LP and PLF) are not necessarily primary products, the data permit the following conclusions to be drawn:

1) Various projectilelike fragments are observed in coincidence with light particles, and coincidence with the conjugate product (PLF=P−LP) is not dominant (Fig. 14). This indicates that transfer processes with subsequent breakup of an excited projectilelike fragment play an important role.

2) Both "elastic" ($E^*_{tot}\approx 0$) and "inelastic" (dissipative) processes of breakup of the incident ion are observed: Figs. 15 and 17. In the $^{83}Nb(^{20}Ne,^{16}O,\alpha)$ reaction, the fraction of elastic breakup of the incident ion (the quasielastic peak in Fig. 15) is remarkably small, being only 25% of the total yield of correlated ^{16}O–α fragments. Note that the ratio depends strongly on the emission angles of the light particle LP and of the conjugate fragment PLF.

3) The energy loss in the process of transfer with subsequent breakup of the primary projectilelike nucleus is much greater than could be expected in a direct few-nucleon transfer process (Fig. 16). The arrow with label Q_{opt} in this figure corresponds to the optimal Q reaction value of the primary two-body process $m_1+m_2\rightarrow m_3+m_4$, obtained under the assumption of direct transfer of nucleons from the projectile to the target without momentum transfer:[46]

$$Q_{opt}=-E_{proj}\frac{m_2(m_1-m_3)}{m_1m_4}\approx 115\ \text{MeV}.$$

In fact, the energy dissipated in the entrance channel is greater by several tens of mega-electron-volts (Fig. 17), and this indicates the existence of additional mechanisms of energy loss in the entrance channel besides the losses associated with the transfer of the nucleons themselves.

Whereas the situation with regard to "elastic" and "inelastic" breakup is more or less clear (both are observed, and their relative importance is determined by the energy and mass of the incident ion and by the emission angles of the fragments), the division into two breakup mechanisms—"direct" and "sequential," in which the incident ion is initially excited and then decays into two fragments—cannot be regarded as unambiguously established. Figure 18 shows one of the first results on the angular correlation of α particles with a projectilelike fragment in the $^{14}N+^{159}Tb$ reaction at $E_{^{14}N}$ = 168 MeV.[11] The asymmetric part of the angular distribution of the α particles is usually interpreted as sequential breakup (decay) of an excited projectilelike fragment.

Figure 19 shows the analogous data for the $^{20}Ne+^{197}Au\rightarrow\alpha+^{16}O+X$ reaction at energy 20 MeV/nucleon.[7] Whereas for small emission angles of the heavy fragment ($\vartheta_{PLF}=25°$, Fig. 19) one can say that sequential breakup does play an important part, for angle $\vartheta=40°$ ($>\vartheta^{in}_{gr}\approx 20°$) the mechanism of nonsequential breakup of the incident ion is clearly dominant in the yield of α particles correlated with a projectilelike fragment. The

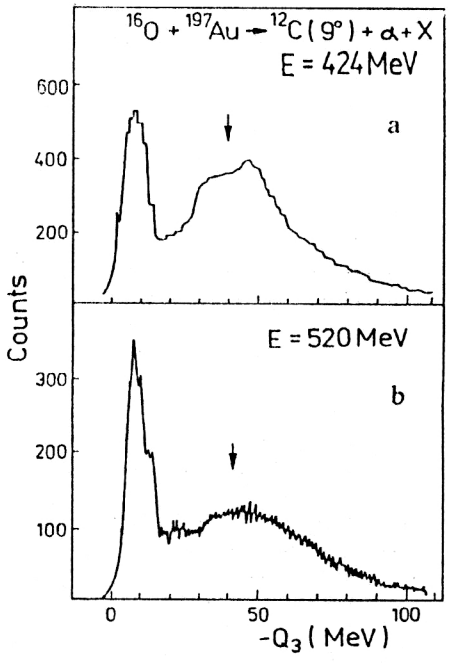

FIG. 17. The Q_3 spectrum for the $^{16}O+^{197}Au \rightarrow \alpha + ^{12}C + X$ reaction. The α particles were detected by phoswich detectors in the region of angles 4–14° in the reaction plane.[59]

predominant energy of the relative motion for the geometry $\vartheta_\alpha = -7°$, $\vartheta_{PLF} = 40°$ is also very large: $E_{opt}^{rel} \approx 20$ MeV.[7]

Finally, Fig. 20 shows the spectrum of the relative motion of the "breakup" fragments in the reaction

$$^{16}O + ^{197}Au \rightarrow \alpha(4 \div 14°) + ^{12}C(9°) + X$$

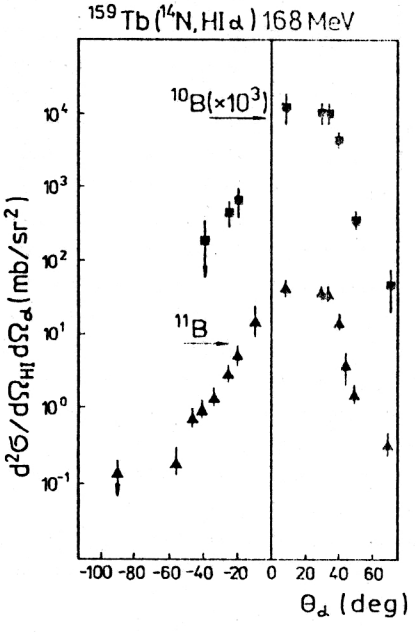

FIG. 18. Angular correlations of α particles and projectilelike fragments in the $^{14}N+^{159}Tb \rightarrow \alpha + PLF + X$ reaction at $E_N^{lab} = 168$ MeV.[11]

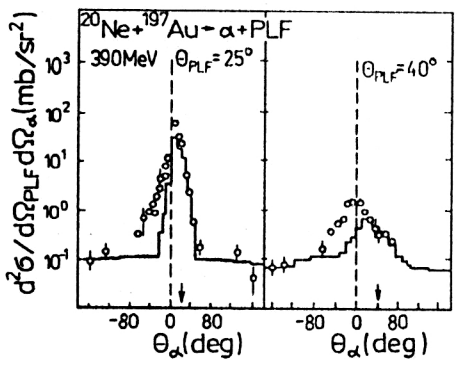

FIG. 19. Double differential cross section of correlated production of α particles and projectilelike fragments with $Z=8$ in the $^{20}Ne+^{197}Au$ reaction at $E_N^{lab} = 390$ MeV.[7] The histogram represents a Monte Carlo simulation of successive breakup of the incident ion.

at energy $E_{^{16}O} = 424$ MeV,[59] which, apparently, gives clear evidence for the mechanism of sequential breakup of an excited projectile $^{16}O^*$; for the peak at $E^{rel}(\alpha, ^{16}O) \cong 4.5$ MeV can be interpreted as decay of the excited 2^+ state at $E^* = 11.47$ MeV in the ^{16}O nucleus[55] (the energy of separation of ^4He and ^{12}C in ^{16}O is $E_{sep} \approx 7.15$ MeV). However, from the experience of the experimental and theoretical analysis of the breakup of the simpler ^2H system we know that in direct breakup the optimum energy of the relative motion is also not equal to zero and is close to the binding energy of the fragments. Note also that the width of the peak in Fig. 20 is fairly broad (the distribution with respect to $E_{rel}^{LP,PLF}$ is in general broader, the greater the inelasticity of the reaction[7,61]), and its position is close to the Coulomb barrier in the interaction of an α particle with ^{12}C. All this (and also the absence of adequate theoretical models) makes it impossible for us to separate unambiguously the fraction of sequential breakup in the joint yield of two projectilelike particles.

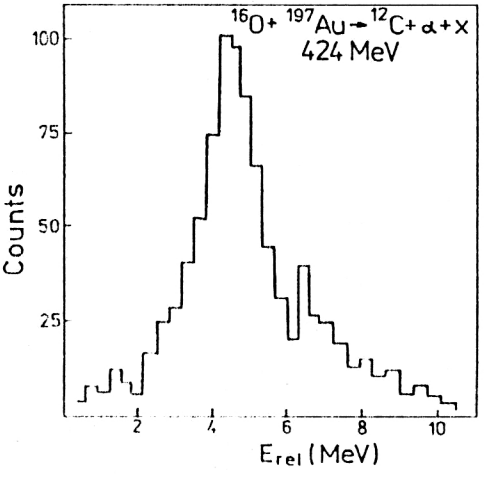

FIG. 20. Energy spectrum of relative motion of the α particle and ^{12}C in the $^{16}O+^{197}Au \rightarrow \alpha(4–14°) + ^{12}C(9°) + X$ reaction at beam energy 424 MeV. The data correspond to the region of the quasielastic peak in Fig. 17a.[59]

TABLE II. Partial cross sections for the production of different fragments (mb/sr) at $E_N^{lab} = 236$ MeV and $\vartheta_{PLF}=20°$ in channels with fixed charge of the final nucleus.

PLF \ Z_{res}	64	65	66	67	68	69	70
α	71	215	290	220	185	140	7
Li	9	23	24	40	15	16	
Be	2	7	20	12	8		
B	6	46	25	57			
C	18	105	158				
N	11	232					

1.6. Coincidence with other light particles (Refs. 8, 26, 35, 36, 65, and 66)

In the studies of Refs. 12–16 [in experiments based on determination of the charge of the final nucleus by means of the characteristic *KX* radiation (see Sec. 1.2)], it was shown that in the $^{14}N+^{159}Tb$ reaction at $E_{^{14}N}$ = 6–22 MeV/nucleon a large proportion of the light particles emitted forward is accompanied by other light particles (with $Z\leqslant 2$) and not by projectilelike fragments (PLF with $Z\geqslant 3$). In fact, neither projectilelike fragments nor other like particles in coincidence with the original light particle were detected in these experiments. Instead, they determined the partial cross sections for production of fragments in coincidence with different final nuclei in the reaction

$$^{14}_{7}N+^{159}_{65}Tb \Rightarrow PLF+B(KX)+X,$$

$$Z_{proj}+Z_{targ}=Z_{PLF}+Z_B+\Delta Z.$$

A typical matrix of such cross sections is given in Table II.

The further analysis of these data is based on the following assumptions.[15]

(a) The yield of projectilelike fragments with $Z_{PLF}\geqslant 3$ in the nonbinary channels with $\Delta Z\neq 0$ is due to p or α decay of a primary excited fragment (with α decay predominating over $2p$ decay). For example, the production of boron in the channel with $Z_{res}=66$ ($\sigma\cong 25$ mb/sr; see Table II) is due to proton decay of a primary excited carbon nucleus. Thus, the total cross section for production of *primary* carbon nuclei is determined, for example, as

$$\sigma^{tot}(C)\approx 158+25+20+24=227 \text{ mb/sr}.$$

(b) The evaporation of charged particles from the primary excited targetlike nucleus B_{pr} can be ignored as a source of processes with $\Delta Z\neq 0$.

Both assumptions [especially (b)] can be challenged. Nevertheless, we give here conclusions based on them[15] which make it possible, at least approximately, to decompose the total cross section for production of light particles into different (admittedly poorly defined) channels. Using assumption (a), we can separate from the complete set of α particles emitted forward in a channel with given Z_{res} the "evaporated" α particles (by simply taking their yield in the same channel at large angles) and the α particles accompanied by a projectilelike fragment with $Z\geqslant 3$. For example the cross section for the production of all α particles (at $\vartheta_\alpha=20°$) in the channel with $Z_{res}=67$ is equal to 220 mb/sr (see Table II). However, the cross section for the production of Li nuclei in the same channel is 40 mb/sr. Assuming that the Li nuclei in the channel with $Z_{res}=67$ ($\Delta Z=2$) are produced by the decay of a primary excited boron nucleus,

$$^{14}_{7}N+^{159}_{65}Tb \Rightarrow {}_{67}B_{pr}+{}_{5}B^{*} \hookrightarrow {}_{3}Li\pm\alpha,$$

we obtain the cross section 40 mb/sr for the production of α particles accompanied by Li nuclei (following Ref. 15, we denote this cross section by σ^{α}_{SD}). The remaining cross section $[220-40-\sigma_{EV}(\alpha)]$ corresponds to the α particles accompanied by only other light particles with $Z=1, 2$.

Figure 21 shows the decomposition of the total cross section for the production of α particles emitted forward into different channels in the reactions $^{14}N+^{159}Tb$ (Ref. 15) and $^{20}Ne+^{159}Tb$ (Ref. 16) obtained in this manner. Figure 22 shows the inclusive yield of α particles (as a sum over final nuclei) as a function of the energy of the incident ion. We see that for comparatively light ions (such as ^{14}N) in the region of energies 6–22 MeV/nucleon the main source of α particles emitted forward is transfer processes ($Z_B > Z_A$) with the appearance in the exit channel of only light particles with $Z\leqslant 1, 2$. Although the fraction of breakup of the incident ion (with a further projectile-like fragment with $Z\geqslant 3$ appearing in the final channel together with the α particle) does increase with increasing initial energy, it does not exceed 25% of $\sigma_{tot}(\alpha)$ (Fig. 21).

Figure 23 shows the partial cross sections of the channels with emission of only light particles ($Z=1, 2$) with different beam energies. We see, thus, that at low energies the binary process of massive transfer with production of only one (nonevaporation) α particle is dominant. With increasing energy, the total multiplicity of the light particles rapidly increases, and it becomes much harder to estimate the contributions of the primary processes in which they are produced on account of the large excitation energy of the primary nuclei.

We emphasize once more that the results presented in Figs. 21–23 were not obtained in a direct experiment but are based on the additional assumptions (a) and (b).

Figure 24 shows the integrated (over the energy) double differential cross section for simultaneous production of two α particles (in one plane) as a function of the angle of

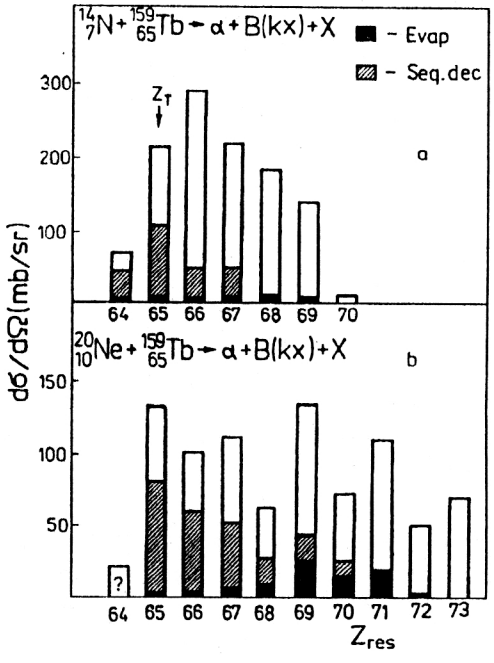

FIG. 21. Partial cross sections for the production of α particles in coincidence with characteristic radiation of the final nucleus (Z_B). The black rectangles represent "evaporated" (isotropic) α particles, the hatched rectangles represent nonequilibrium α particles accompanied by projectilelike fragments with $Z \geq 3$, and the remaining part corresponds to channels in which only light charged particles with $Z \leq 2$ are observed. a) The ^{159}Tb(^{14}N,α) reaction at beam energy 236 MeV and $\vartheta_\alpha = 20°$ (Ref. 15); b) the ^{159}Tb(^{20}Ne,α) reaction at $E_{Ne} = 294$ MeV and $\vartheta_\alpha = 25°$ (with correction for evaporation of charged particles).[16]

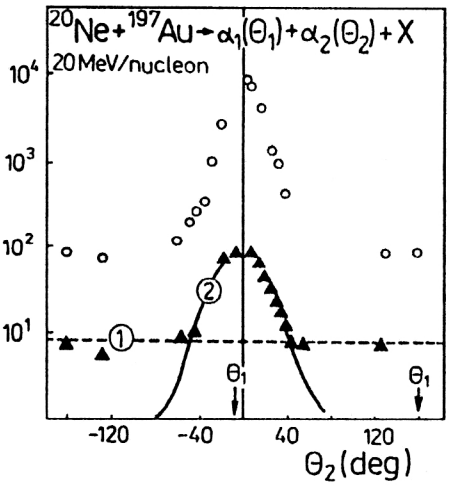

FIG. 23. Partial cross sections of channels in which only light charged particles (equilibrium and nonequilibrium) with charge $Z=1$ and 2 are emitted. The presumed combinations of emitted light particles are indicated at the bottom.[15]

one of them for fixed (forward and backward) angle of the other. Using these data, it is possible to estimate the contribution of the various processes to the inclusive production of α particles[8] (the total simultaneous yield of two α particles in this reaction is 1100 mb).

1) *Complete fusion* with evaporation of two (or more) α particles can be extracted from the isotropic part of the angular distributions (the "platform" for the case $\vartheta_{\alpha_1} = 160°$): $\sigma(CF \rightarrow 2\alpha) = 400 \pm 50$ mb. This value can be compared with the total fusion cross section, which is estimated[3] for this reaction to be 800 mb.

2) *Incomplete fusion* with one α particle emitted forward and fusion of the remnant (here ^{16}O) with the target and *subsequent* evaporation of a further α particle. The cross section of this process can be estimated by integrating the forward peak of the elastic distribution at $\vartheta_{\alpha_1} = 160°$ (Fig. 24) (under the assumption of an isotropic angular distribution of the evaporated particle α_2): σ_{ICF} (1α forward $+ 1\alpha$ evaporated) $= 500 \pm 60$ mb. These two processes almost exhaust ($2 \times 400 + 500$) mb the total cross section for the production of all evaporated α particles, which for this reaction is estimated[8] to be 1600 mb.

The role of the remaining possible sources of simultaneous production of two α particles (decay of ^{8}Be, ^{12}C*,

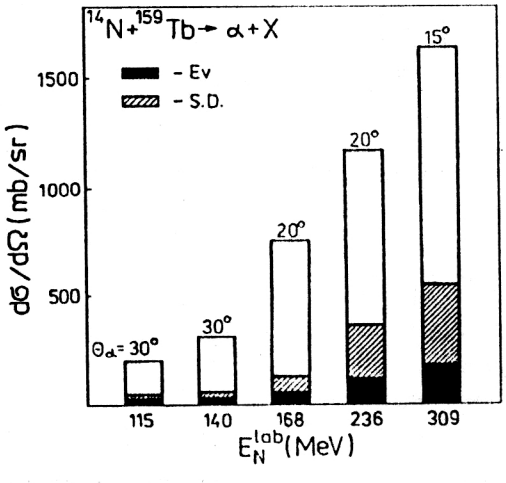

FIG. 22. Decomposition of the inclusive yield of α particles at forward angles in the ^{14}N+^{159}Tb reaction into three components (the notation is the same as in Fig. 21).[15]

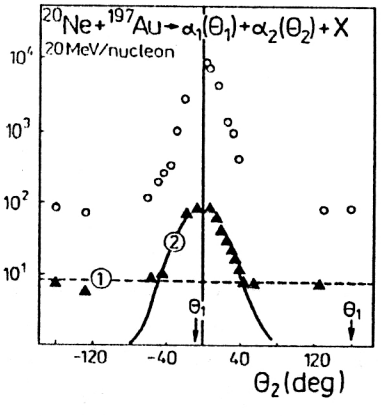

FIG. 24. Integrated (over the energy) double differential cross section for simultaneous production of two α particles in the ^{20}Ne+^{197}Au $\rightarrow \alpha_1(\vartheta_1)+\alpha_2(\vartheta_2)+X$ reaction at beam energy 20 MeV/nucleon. The laboratory emission angle of the first α particle is indicated by the arrow: $\vartheta_{\alpha_1} = -7°$ (open circles), $\vartheta_{\alpha_1} = 160°$ (black triangles).[8]

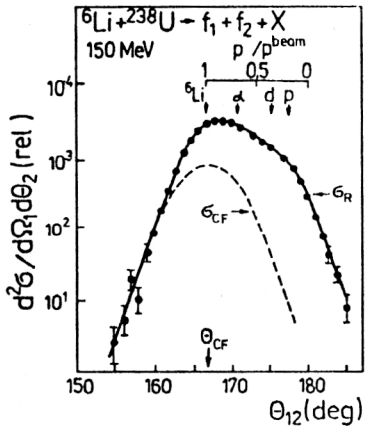

FIG. 25. Inclusive yield of fission fragments in the $^6Li+^{238}U$ reaction at $E_{^6Li} = 150$ MeV as a function of the emission angle. The arrows show the optimum emission angles for transfer to the target nucleus of one nucleon, a deuteron, or an α particle, and also for complete fusion of the nuclei. The broken curve is the upper limit of the cross section for complete fusion obtained from the angular distribution out of the reaction plane.[72]

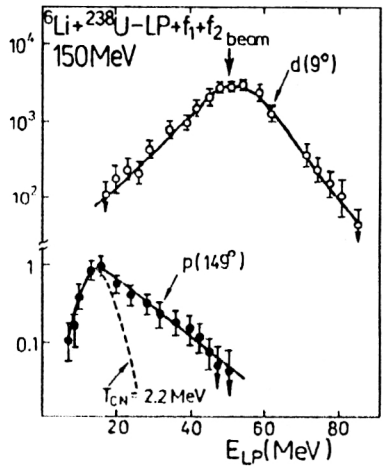

FIG. 26. Energy spectrum of deuterons and protons in coincidence with fission fragments in the $^6Li+^{238}U \rightarrow LP+f_1+f_2$ reaction at beam energy 150 MeV. The broken curve is the calculated evaporation spectrum of protons under the assumption of complete fusion of the nuclei ($T=2.2$ MeV).[72]

etc.) cannot be estimated so obviously,[8] and therefore we give here only the corresponding numbers. Finally, we note that the comparatively large cross section of the process (2) casts doubt on the assumption (b) (see above) made in Ref. 15.

1.7. Coincidence with fission fragments and detection of heavy residual nuclei (Refs. 23, 26, 39, and 67–81)

From the emission angle of the fission fragments of a heavy final nucleus in coincidence with a light particle one can readily deduce the momentum tranfer Δp_{tr} to the heavy nucleus, i.e., one can deduce the nature of the reaction in which the light particle was produced, namely, if $\Delta p_{tr}=p_{beam}$, then we have a complete fusion process, if $\Delta p_{tr}<p_{beam}$ an incomplete fusion process, and if $\Delta p_{tr}\approx 0$ a grazing collision with subsequent quasielastic breakup of the projectile.

We consider first a simpler experiment of this kind with a light incident ion. Figure 25 shows the inclusive yield of fission fragments from collisions of ^6Li with ^{238}U at $E_{^6Li} = 150$ MeV as a function of the emission angle.[72] Figure 26 shows the energy spectra of deuterons and protons in coincidence with fission fragments. The maximum of the spectrum for forward emission angles exactly corresponds to the velocity of following, and this is usually interpreted as indicating a dominant role of incident-ion breakup processes. However, in this case it was established quite definitely (see below) that the main source of deuterons in this reaction was the process of "massive transfer" of an α particle from the projectile to the nucleus. This fact must make us wary of conclusions based on general arguments but not supported by direct experiment. Note also that in the case of light ions such as ^6Li the role of dissipative processes is much less important if one judges from the sharp decrease of the cross section at $v_{PLF} < v_{beam}$ for small angles.

Figure 27 shows the yield of fission fragments of the final nucleus in coincidence with deuterons as a function of the momentum transfer to the final nucleus as determined from the fragment emission angles. Of the two main sources of deuterons in this reaction—the breakup process $^6Li \rightarrow \alpha+d$ and the incomplete-fusion process $^{238}U(^6Li, d)$—the former is the dominant one. Breakup of the incident ion makes a certain contribution only in the region of the most forward angles. Note also that the relative importance of the incomplete-fusion channel becomes ever greater not only with increasing angle but also with increasing energy of the light particles.[72]

In the analysis of such reactions, a convenient characteristic quantity is

$$R=\frac{p^{\parallel}(\mathrm{LP})+p^{\parallel}(f_1f_2)}{p_{\mathrm{beam}}},$$

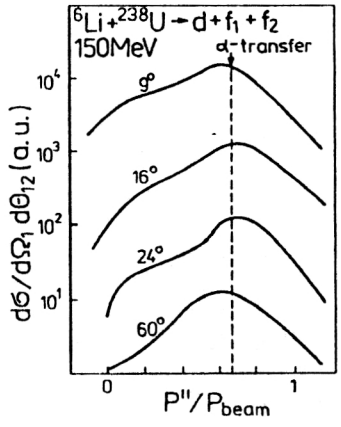

FIG. 27. Yield of fission fragments in coincidence with a deuteron in the $^{238}U(^6Li, df_1f_2)$ reaction as a function of the momentum transfer to the final nucleus. The broken line corresponds to transfer of an α particle to the nucleus.[72]

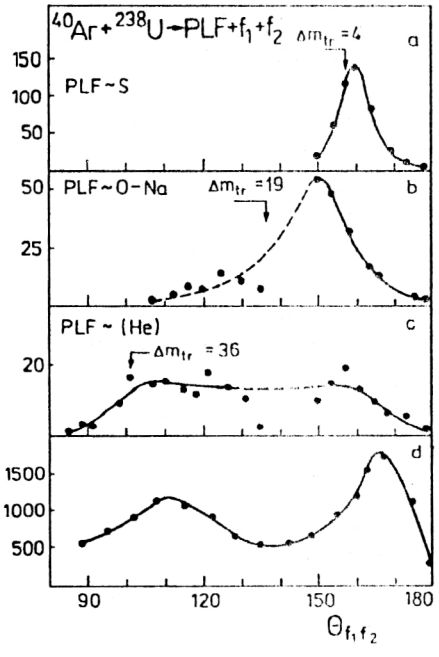

FIG. 28. The $^{40}Ar+^{238}U \rightarrow PLF+f_1+f_2+X$ reaction at $E=27$ MeV/nucleon. The correlation function of the fission fragments in coincidence with projectilelike fragments detected at $\vartheta_{PLF}=8°$ (a–c) and their total yield (d) as functions of the emission angle. The arrows show the optimum emission angles of the fission fragments under the assumption of a two-body incomplete-fusion reaction. The curves are drawn for clarity.[75]

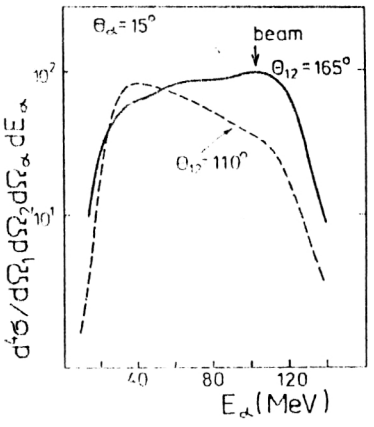

FIG. 29. Energy spectra of α particles in coincidence with two fission fragments emitted in the same plane with emission angles $110\pm6°$ and $165\pm6°$, $\vartheta_\alpha=15°$. For clarity, only the curves drawn through the set of experimental points are shown.[75]

where $p^{\parallel}$ (LP) and $p^{\parallel}$ (f_1f_2) are the longitudinal components of the momentum of the light particle and of the fission fragments. If R is close to unity, this means that the particles participating in the reaction have been completely taken into account. In this case, the mean value $\langle R\rangle$ is close to unity for emission of deuterons in the entire forward region of angles (and this confirms once more the dominant role of the α-particle stripping channel), and $\langle R\rangle \approx 0.84$ for emission of protons. This value corresponds to the loss of one nucleon (with velocity of the beam), and it indicates the importance of the channel

$$^{6}_{3}\mathrm{Li}+^{238}_{92}\mathrm{U} \rightarrow (^{242}\mathrm{Pu}+d) \rightarrow ^{252}\mathrm{Pu}+p+n$$

in the production of protons.[72] One further distinctive feature of proton production is the extremely hard (i.e., clearly not evaporation) proton spectrum at backward angles, showing that the assumption of an evaporation nature of all light particles at backward angles is by no means always correct.

Analysis of similar reactions initiated by heavier incident ions is undoubtedly much more difficult because of the greater multiplicity of the produced light particles. Obviously, it most convenient to perform such experiments using 4π detectors with analysis of each event separately, for this would not only permit determination of the relative importance of the individual reaction channels but also make it possible to determine the absolute values of their cross sections.

Figure 28 shows the inclusive yield of fission fragments and also their coincidences with different projectilelike fragments emitted forward as a function of the emission angle of these fragments. We see that in the yield of fragments having mass close to the projectile mass two-body transfer processes in which the projectile remnant (I–PLF) fuses with the target are predominant. In contrast, in the production of light fragments an important role is played by processes in which a significant fraction of the initial momentum is carried away by particles that do not fuse with the target and are not detected in the experiment. As a result, in the inclusive yield of fission fragments (Fig. 28d) at a given energy one can clearly observe two peaks corresponding to fusion (complete or incomplete) processes with $\Delta p_{tr} \approx p_{beam}$ (the maximum at $\vartheta_{f_1f_2} \approx 110°$, $\Delta p_{tr}/p_{beam} \approx 80\%$) and collision processes with small momentum transfer (the maximum at $\vartheta_{f_1f_2} \approx 165°$, $\Delta p_{tr}/p_{beam} < 10\%$).

The spectra of α particles in coincidence with fragments at $\vartheta_{f_1f_2} \approx 110°$ and 165° are shown in Fig. 29. In contrast to the reactions with light ions (see above), in the given case more energetic α particles are emitted in grazing collisions with small momentum transfer. Note, however, that here the spectrum of α particles only in the region of the velocity of following was measured. It would be interesting to compare the hardest part of the spectrum of light particles in reactions with small (grazing fragmentation processes) and large (more central, incomplete-fusion processes) momentum transfer.

With increasing energy, one observes here an interesting effect of weakening of transfer processes and disappearance of the corresponding component in the angular correlations of the fission fragments. Figure 30 shows the corresponding distributions in the $^{40}Ar+^{197}Au$ reaction at energy $E=35$ MeV/nucleon (when the incomplete-fusion processes can still be clearly seen) and at $E=44$ MeV/nucleon.

From the position of the maximum at $\vartheta_{f_1f_2} \approx 94°$ ($E=35$ MeV/nucleon) it may be concluded that there is a ~74% transfer of the projectile momentum, corresponding approximately to a momentum 188 MeV/c per incident

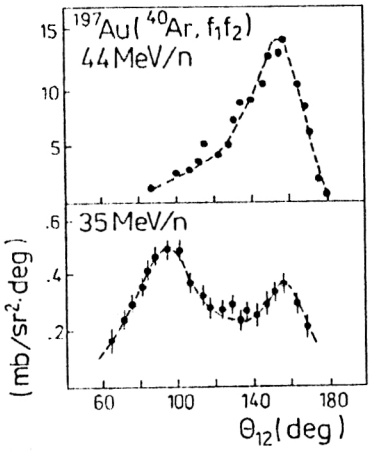

FIG. 30. Angular correlations of fission fragments in the $^{40}Ar+^{197}Au$ reaction at $E=35$ MeV/nucleon[71] and $E=44$ MeV/nucleon.[82]

nucleon. Observations of this kind have led to the assumption that there is a certain limiting momentum transfer ($\sim$180–190 MeV/c per incident nucleon) that is independent of the collision energy (at least in the region 27–44 MeV/nucleon) and of the excitation energy of the final nucleus.

Another possibility for determining the longitudinal momentum transfer in the reaction is to measure the velocity distributions of heavy residual nuclei. Figure 31 shows the inclusive velocity distribution of all heavy residual nuclei, and also their distribution in coincidence with α particles in collisions of 313-MeV ^{16}O nuclei with ^{40}Ca.

The spectrum of the velocities of the heavy residual nuclei (inclusive and in coincidence with α particles emitted forward) is shifted to lower velocities compared with the velocity of the compound nucleus that could be produced in a complete-fusion process. This means that incomplete-fusion or massive-transfer processes are predominant. Analysis of such spectra can give information on the fraction of the incident ion that is stripped on the target nucleus. In particular, it was concluded in Ref. 77 that the shift of the spectrum of velocities of heavy recoil nuclei in coincidence with fast α particles emitted forward relative to the velocity of a compound nucleus was too large. This can be explained by assuming that the main source of fast α particles in this reaction is the process of massive transfer, not to ^{12}C, but only to ^{8}Be with subsequent decay of another ^{8}Be nucleus emitted forward.

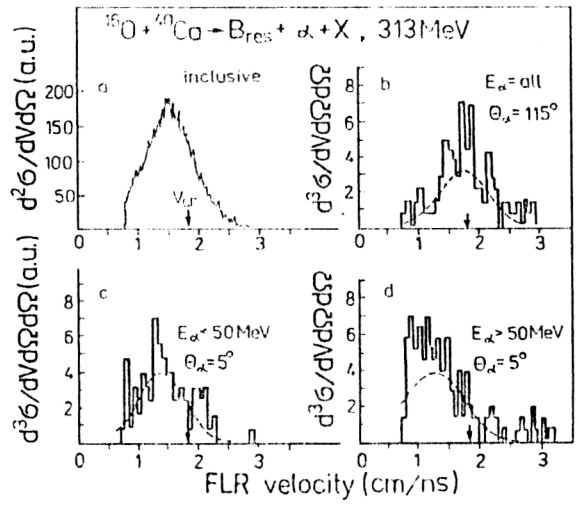

FIG. 31. Spectrum of velocities of heavy residual nuclei detected at angle $\vartheta_{HR}=15°$. The histograms represent the experiment; the continuous curves are fitted Gaussians. a) Inclusive spectrum; b) coincidences with α particles emitted at angle 115°; c) coincidences with α particles with energy less than 50 MeV (i.e., with velocities less than the beam velocity) at $\vartheta_\alpha=5°$; d) coincidences with α particles with $E_\alpha>50$ MeV ($v_\alpha \geqslant v_{beam}$) at $\vartheta_\alpha=5°$. The arrow indicates the velocity of the compound nucleus under the assumption of complete fusion.[77]

2. WHAT IS USUALLY ASSUMED (ALTHOUGH NOT EXPLICITLY PROVED AND SOME DOUBTS REMAIN)

2.1. Evaporation of light particles

The fraction of evaporated light particles is always determined in the simplest manner—by assuming that all particles emitted at backward angles are evaporation products and that their angular distribution is isotropic. Such a procedure usually leads to the conclusion that approximately half of all the α particles produced in heavy-ion collisions in the range of energies from 5 to 30 MeV/nucleon is due to evaporation from a heavy final nucleus (see, for example, Ref. 13 or Ref. 3 with allowance for the conversion in Ref. 8), although for forward angles the fraction of evaporation α particles is negligibly small ($\leqslant$5% at $E\sim$20 MeV/nucleon). These conclusions are assumed to be entirely reliable and, as a rule, are not discussed.

We wish to note here that not only light particles can be emitted at backward angles but also fragments produced in the initial stage of the reaction, before complete thermodynamic equilibrium is achieved in the compound nucleus. This is manifested particularly clearly at not too high energies ($\leqslant$10 MeV/nucleon). Calculations show that even in direct single-step massive-transfer processes the light particles are directed predominantly backward at near-barrier energies $E-V_C^B \leqslant 1.5$ MeV/nucleon; their angular distribution is practically isotropic at $E-V_C^B \sim$ 1.5–2.5 MeV/nucleon, and only at high energies does it become forward directed, preserving a nonzero value at backward angles.[83] With increasing energy, the direct mechanisms of production of light particles naturally lead to an ever greater forward directionality. However, the dissipative processes that decelerate the incident ion, and also the potential forces of the mean field, leading to deflection through appreciable angles of both the projectile in the entrance channel and the projectilelike fragment in the exit channel, can very well lead to a significant yield of nonequilibrium light particles at large angles.

Thus, the estimate of the importance of the evaporation processes in the production of light particles based on their yield at backward angles may be overestimated, especially in the region of energies $\leqslant$10 MeV/nucleon. There is still more doubt about the existence of an energy thresh-

old (~5 MeV/nucleon above the Coulomb barrier) in the production of nonequilibrium α particles.[3] However, there does not appear to be any possibility (except by theoretical calculations) of distinguishing slow nonevaporation particles from slow evaporation particles.

2.2. Role and mechanism of the breakup process

The breakup of the incident ion into two light fragments ($I \rightarrow a+b$) in the field of the target nucleus can be recognized as elastic or inelastic in accordance with the amount of kinetic energy dissipated in the reaction (see Figs. 15 and 17) and as direct (occurring immediately in the field of the target nucleus A with "three-particle" dynamics $V_{aA}+V_{bA}+V_{ab}$) or sequential (due to the interaction V_{ab}) breakup of an excited ion I^* far from the target nucleus. Thus, one can separate the contributions of the four different breakup processes in the yield of light particles a; the elastic and inelastic components can be separated fairly reliably (see Sec. 1.5), but the separation into the direct and sequential mechanisms is more uncertain. It is often asserted (Refs. 2, 7, 9, 11, 59, and 61) that it is the inelastic processes of sequential breakup of an excited ion I^* that is dominant (although opposite assertions are also made[65,84]). Such a conclusion is usually based on the energy spectrum of the relative motion E_{ab}^{rel} of fragments a and b (see Sec. 1.5). However, as already noted, the behavior of the relative motion of the fragments is rather similar in the direct and sequential breakup processes, and it is very difficult, if it is possible at all, to separate them on the basis of this characteristic. In addition, it was shown in Refs. 7 and 61 that at energies 20–40 MeV/nucleon the spectrum of the relative motion of the breakup fragments clearly contains a component with large values of E_{ab}^{rel} that can in no way be associated with a mechanism of sequential breakup.

Thus, we can do no more than state the following fact: Both *direct* and *sequential* breakup of the incident ion in the field of the target nucleus are possible; at the present time it is not possible to establish unambiguously the fractions of the two mechanisms as functions of the mass and initial energy of the projectile and of the fragment emission angles.

Another problem that has not been finally solved is that of the relative contribution of all the breakup mechanisms to the total yield of light particles, i.e., the problem of the total cross section for the process of breakup of the incident ion. Here too there are different points of view, based on incomplete experimental data and additional model assumptions. If an unambiguous conclusion is to be drawn about the total cross section for breakup of the incident ion, it is necessary to integrate over all emission angles of the fragment conjugate to the light particle (in the reaction plane and out of the reaction plane). It is clear that it is practically impossible to do this without the use of 4π detectors.

To establish the relative contributions of the pure breakup (fragmentation) process and transfer processes to the yield of projectilelike fragments, the study of Ref. 57 used a wall of 72 plastic detectors that covered the range of angles from 3° to 30° and detected (with identification of the charge) all light particles with $Z \leqslant 8$ in coincidence with a projectilelike fragment in the $^{40}Ar+Ag$ reaction at energy 35 MeV/nucleon. Figure 32 shows the results of such coincidences for $Z_{PLF}=16$; they indicate that even at such a high energy it is the transfer reactions (yield of PLF without accompanying light particles) and not fragmentation processes that are dominant. Note that some of the light particles with $Z=1$ and $Z=2$ observed in coincidence with PLF may have an evaporation origin (this could be established by cutting out the light particles with low energy), so that the fraction of the primary two-body transfer process may be even larger. The experiment indicates that the so-called fragmentation peaks observed in the inclusive spectra of the light particles (at energies corresponding to the beam velocity) may in fact have a more complicated nature.

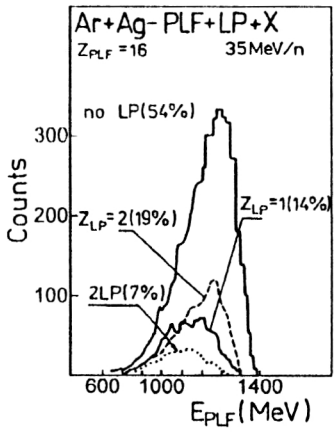

FIG. 32. Energy spectrum of projectilelike fragments (PLF) with $Z=16$ emitted at angle $\vartheta_{PLF}=5°$ in coincidence with light particles.[57]

2.3. Weakening of dissipative processes with increasing energy

It is assumed that in heavy-ion collisions at low energies ($\leqslant$20 MeV/nucleon) deep inelastic processes with considerable dissipation of the kinetic energy of the relative motion are dominant, while the dissipative processes are manifested less strongly at higher energies ($\geqslant$40 MeV/nucleon). This is manifested in the yield of light particles in a displacement of the maximum of their spectrum ever closer to the velocity of following with increasing energy of the incident ion (see Sec. 1.1). However, despite a general trend of this kind, the maxima of the light-particle spectra always occur at $v_{LP} < v_{beam}$ at energies up to 100 MeV/nucleon, and, in addition, a low-energy "dissipative" part is always observed in these spectra, being the greater, the greater the mass loss and the larger the emission angle of the light particles, i.e., the larger the momentum transfer.

Figures 33 and 34 show the spectra of light projectilelike fragments in the $^{40}Ar+^{68}Zn$ reaction at $E=20$ and 35 MeV/nucleon[85] and in the $^{40}Ar+^{238}U$ reaction at $E=100$ MeV/nucleon.[86]

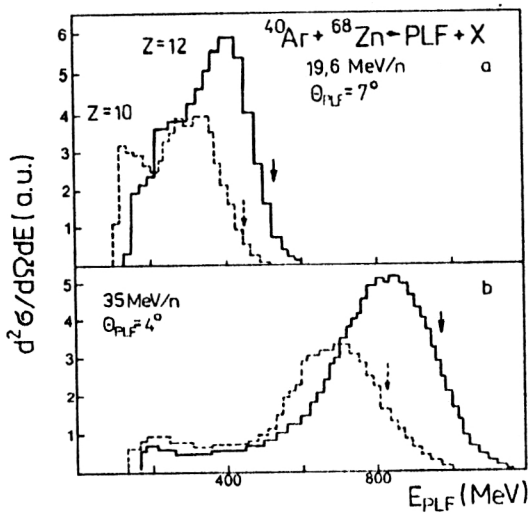

FIG. 33. Energy spectra of projectilelike fragments (with $Z=10$ and $Z=12$) in the $^{40}Ar+^{68}Zn$ reaction at $E=19.6$ MeV/nucleon (a) and 35 MeV/nucleon (b). The arrows indicate the energies corresponding to the beam velocity.[85]

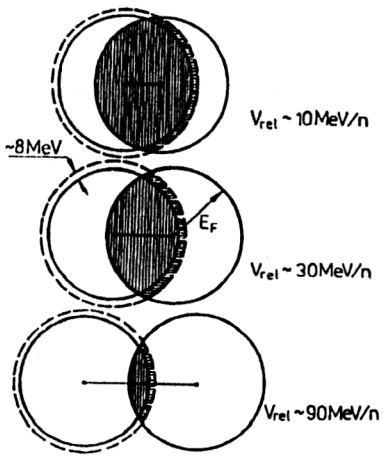

FIG. 35. Position of the two Fermi spheres reflecting the momentum distribution of the nucleons in the target and projectile for different energies of their relative motion. The broken circle corresponds to the upper limit of bound states of nucleons in the target ($\sim E_F+8$ MeV).[87]

Thus, with increasing energy ($\geqslant$40 MeV/nucleon), "fragmentation" processes of breakup of the incident ion become more and more significant, although a low-energy component, which it is most natural to associate with dissipative processes, can clearly be observed in the spectrum of projectilelike fragments and light particles. There arises in this connection one of the basic problems of heavy-ion physics: Up to what velocities of the relative motion can one speak of nuclear friction, what is the rate (or time) of dissipation, and, finally, what is the mechanism of dissipation of the energy of the relative motion at low and high velocities?

2.4. Disappearance (weakening) of transfer processes with increasing energy

Figure 35, which is taken from Ref. 87, shows schematically in the momentum space the Fermi spheres of the projectile and target for different velocities of the relative motion. The radius of the broken circle corresponds to the energy ($\sim E_F+8$ MeV) of the last bound state of a nucleon in the target. The shaded region of overlap of the two spheres reflects the role of blocking (due to the Pauli principle), which becomes smaller and smaller with increasing energy. Finally, the narrow hatched region corresponds to quasielastic processes of stripping of nucleons to bound states of the target. It can be seen from the figure that the cross sections of such transfer processes must become smaller and smaller with increasing energy of the incident ion. This conclusion is supported, for example, by data on the yield of fragments of fission of the final nucleus (Fig. 30), which show that the component corresponding to processes of complete and incomplete fusion (large momentum transfers) gradually disappears with increasing energy. As regards the yield of light particles, this means that at energies $\geqslant$100 MeV/nucleon the main mechanism of their production must be the mechanism of breakup (fragmentation) of the incident ion, and stripping processes (including the process of incomplete fusion) can be completely ignored.

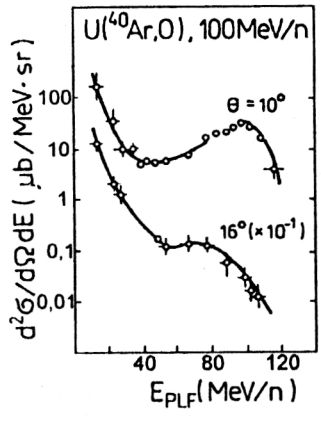

FIG. 34. Energy spectrum of oxygen nuclei in the U(^{40}Ar, O) reaction at $E=100$ MeV/nucleon for two emission angles greater than the angle of a grazing collision.[86]

However, if at energies $\sim$100 MeV/nucleon dissipative processes still play some role, the arguments based on the separation of the two Fermi spheres become invalid, since, first, the Fermi distributions in both nuclei become appreciably smeared as their excitation energy increases and, second, the separation is significantly reduced by the decrease in the velocity of the relative motion. Thus, experiments to detect transfer processes (and establish their total cross section) in the region of energies $\sim$100 MeV/nucleon are of great interest. Such processes can be clearly identified by detecting, for example, fission fragments with charge $Z_1+Z_2>Z_{targ}$ or by recording all projectilelike fragments and nonevaporation light particles with total charge less than the charge of the incident ion.

3. THEORETICAL MODELS

A systematic quantum-mechanical calculation of the yield of light particles in heavy-ion collisions is impossible in view of the many-particle and many-channel nature of the problem. This is the reason why a rather large number of semimicroscopic or completely empirical approaches based on simplified models have been proposed. Of course, none of these models can explain quantitatively all the observed properties, including the absolute values of the differential cross sections. This status of the theory aggravates the already appreciable uncertainty in the interpretation of the available experimental data, as a result of which it is not possible to make reliable predictions with a view to the planning of new experiments. However, we cannot extract any quantitative information unless we analyze the experimental data in the framework of some theoretical model. It is better to have a bad theoretical model than none at all (if only in order to recognize that it is bad).

3.1. Fermi distribution and Goldhaber model[88]

In this very simple model, it is assumed that the target nucleus plays the role of a spectator in the process of breakup (fragmentation) of the incident ion I, sustaining the energy conservation law. Knowing the momentum distribution of the nucleons in the projectile, we can calculate the analogous distribution for any projectilelike fragment formed randomly from the nucleons of the incident ion. In such a case, the momentum distribution of the fragment is determined by the expression

$$W(p)\sim\exp\left(-\frac{p^2}{2\sigma^2}\right), \tag{1}$$

where

$$\sigma^2=\sigma_0^2\frac{A_I(A_I-A_a)}{A_I-1}, \tag{2}$$

with reduced width $\sigma_0=P_F/\sqrt{5}$, where P_F is the Fermi momentum. It is obvious that the differential cross section for production of the particles a will have a maximum at angle 0° and at energy corresponding to the beam velocity. The single governing parameter of this model is the width σ_0 of the momentum distribution, and this can be found from independent experiments on electron scattering by nuclei or from experiments on high-energy fragmentation of the incident ion. The width is found to be 90–95 MeV/c, in good agreement with the model representation of the momentum distribution of the nucleons in a nucleus.

At $E\leqslant 100$ MeV/nucleon, this simplified approach is not very effective, this being reflected in the need to decrease sharply the value of σ_0 extracted from fitting the energy spectra of the projectilelike fragments when the energy of the incident ion is reduced (down to $\sigma_0\sim 20$ MeV/c at $E\sim 10$ MeV/nucleon). The obvious reason for this is the neglect of the dynamics of the process, i.e., the neglect of the realistic interactions of the fragments a and $b=I-a$ with each other and with the target nucleus, which lead to a significant change of their angular and energy distributions.

3.2. Friedman's model[89]

In Friedman's semiempirical approach, it is assumed that because of "absorption" effects the fragment a is formed only from the outer nucleons of the incident ion I, and its momentum distribution in the projectile is determined, not by the Fermi distribution of the nucleons, but by the wave function in the peripheral region:

$$\Psi_a(r)\sim\frac{e^{-\mu r}}{r}, \tag{3}$$

i.e., ultimately by the energy of separation of fragment a from the nucleus I: $\mu=((2\mu_a/\hbar^2)E_s)^{1/2}$, where $\mu_a=m_a(m_I-m_a)/m_I$ is the reduced mass. Assuming that $F(r)\Psi(r)$, where $F(r)$ models the absorption at small distances, reaches a maximum at a certain x_0, and approximating this quantity by a symmetric Gaussian near x_0, we can calculate the corresponding momentum distribution, the width of which is determined by

$$\sigma^2=\frac{\mu}{2x_0}\left[1+\frac{1}{\mu x_0}\right], \tag{4a}$$

or, with allowance for Coulomb corrections,

$$\sigma^2=\frac{\mu}{2x_0}\left[\frac{1+\frac{y}{2}}{\sqrt{1+y}}+\frac{1}{\mu x_0}\right], \tag{4b}$$

where $y=Z_a(Z_I-Z_a)e^2/x_0E_s$.

The widths (4b), determined by the cluster separation energy E_s and the cutoff radius x_0, which depends on the size of the cluster, is somewhat smaller than (2) and, therefore, closer to the fitted (experimental) values, including those at low energies.

Developing this "peripheral" philosophy, Friedman proposed to describe the relative yield of fragments by means of the expression

$$\sigma(a)\sim S_a|\tilde{\Psi}_a(x_0^a)|^2, \tag{5}$$

where $S_a=Z_I!N_I!/Z_a!Z_b!N_a!N_b!$ is the spectroscopic factor of the fragment in the projectile I ($b=I-a$, and $Z_{a,b,I}$ and $N_{a,b,I}$ are the corresponding numbers of protons and neutrons). The wave function in the peripheral region has the form

$$|\tilde{\Psi}_a(x_0^a)|^2=\frac{\exp[-2\mu_a(x_0^a-R_0^a)]}{R_0^a(x_0^a)^2}, \tag{6}$$

where R_0^a (which is somewhat less than the cutoff parameters x_0^a) ensures correct normalization of the wave function. Using for R_0^a the expression $R_0^a=(1-\beta)x_0^a$ with $\beta=0.4$ for all fragments and suitable fragment separation energies, Friedman obtained a satisfactory description of the relative yields of isotopes in the reaction with ^{16}O at 2 GeV/nucleon.

The shortcomings of this approach include, as before, the complete neglect of the dynamics of the process. In this approach, it is impossible to obtain a realistic description of the angle and energy distributions (and not merely the widths) of the projectilelike fragments, especially at ener-

gies $E \leqslant 100$ MeV/nucleon. From the isotope distributions and the fitted widths σ^2 one can extract quantitatively only x_0^a and R_0^a, which give little information (from the point of view of the internuclear interaction). However, the general conclusion that allowance for the peripherality in reactions with a yield of projectilelike fragments improves the agreement with experiment clearly warrants attention.

3.3. Model of moving sources[86,90]

In this empirical model, it is assumed that the light particles are evaporated isotropically from a source moving parallel to the beam velocity. It is also assumed that there can be several such sources ($i=1,2,...,v$), and that their temperatures T_i and velocities v_i differ and are adjustable parameters (together with normalization coefficients N_i) to be determined by reproducing the experimental energy spectra by means of the following expression for the double differential cross section:

$$\frac{d^2\sigma}{d\Omega dE} = \sum_{i=1}^{v} N_i \sqrt{E-V_c} \times \exp\{-[E-V_c+E_i-2\sqrt{E_i(E-V_c)}\cos\vartheta]/T_i\}, \quad (7)$$

where $E_i=\frac{1}{2}mv_i^2$, m is the mass of the emitted light particle, V_c is its Coulomb energy, and ϑ is the emission angle.

It is obvious that, using several exponentials (7), we can always reproduce sufficiently well the energy spectra (see, for example, Refs. 24, 26, 85, and 86). This model can reproduce especially well the spectra of the nucleons and, somewhat worse, the spectra of complex fragments, for which it is not possible to describe simultaneously the energy and angle distributions. As a rule, at low energies, up to 100 MeV/nucleon, three different sources are found as a result of fitting: one with velocity close to the velocity of the center of mass, which is interpreted as evaporation from a compound nucleus, and two others with higher velocities and higher (often, unphysical) "temperatures" T_i. However, by using one set of sources it is not possible to reproduce the yields of all light particles—for each particle species, it is necessary to choose a new set of sources with new values of their velocities and "temperatures," and the greater the mass of the light particles, the higher the "temperature" and the lower the velocity of the fast sources that are needed.

The weakest point in this empirical model is the interpretation of the quantitative parameters v_i and T_i that are deduced from it. The large values of these quantities indicate that there must be comparatively few nucleons in the "heated" zone. However, the attainment of even local thermodynamic equilibrium in a system of two tens of nucleons (with allowance for the nucleon mean free path $\lambda \sim R_{\text{nucleus}}$ in the nucleus) appears very doubtful. It should be noted that the direct (fundamentally nonstatistical) processes also exhibit exponential dependences, for example, on the momentum transfer. The inclusive nature of the experimental spectra, including a sum over a large number of intermediate channels, smooths still further the behavior of such processes (see below). This means that fast nonequilibrium transfer processes or processes of breakup of the incident ion are probably what is hidden behind the fast "high-temperature" sources. Therefore, one must approach with great care the interpretation of the parameters v_i and T_i of the "moving sources" that are extracted by fitting the experimental data.

3.4. Direct processes (Refs. 83 and 92–97)

The possible important role of direct processes in the production of fast light particles was first argued in some depth in Refs. 92 and 93. In these and other studies, it was proposed to interpret the yield of light particles directed forward as the result of the well-known direct stripping reactions ("massive transfer" and "incomplete fusion") or the breakup of the incident ion, these being described by the standard method of distorted waves. Certain simplifications in such an approach can be achieved by assuming extreme peripherality of such processes and by the possibility of summing over unobservable states of the final nucleus and of the fragment conjugate to the light particle (inclusivity of the reaction). Nevertheless, the final expressions were too complicated to allow their calculation directly by means of the standard programs of the distorted-wave method—the large masses and high energies of the fragments participating in the reaction make it necessary to take into account hundreds of partial waves in the entrance and exit channels and to sum over a large number of angular-momentum transfers in the reaction. In Refs. 93, 96, and 97, the partial-wave amplitudes of the distorted-wave method were simply parametrized, and in Refs. 82, 92, 94, and 95 the semiclassical approximation in three-dimensional space developed for the description of direct nuclear reactions with the participation of heavy ions[98] was used. It was shown that at energies ~ 10 MeV/nucleon the properties of the *direct* processes of massive transfer and breakup agree in principle with the experimental data on the yield of high-energy light particles emitted forward, the stripping process dominating over the breakup process at the hardest end of the spectrum (near the two-body kinematic limit).

Two basic shortcomings are inherent in the explanation of the yield of light particles by means of direct mechanisms. The first is associated with the very hypothesis of a single-step nature of the reaction (summation over the unobservable final states does not at all mean that the many-channel state of affairs is taken into account). It is well known that in heavy-ion collisions at low energies dissipative deep inelastic processes are dominant. It is therefore natural to expect that in the production of light particles too an appreciable role will be played by multistep processes with mutual excitation of the colliding nuclei, and in these processes the light particle may be emitted (by a stripping or breakup process) at any stage in the reaction—from the very beginning (truly direct process) to the stage of complete relaxation of the kinetic energy of the relative motion (see the following subsection). The second shortcoming is the complexity of the prediction of the absolute values of the differential cross sections of the

direct processes resulting from the impossibility of estimating correctly the spectroscopic factors of the complex fragments (we also do not known their experimental values) and the large uncertainty in the choice of the optical potentials that determine the distorted waves in the entrance and exit channels.

3.5. Multistep (dissipative) processes of massive transfer and breakup[99,100]

In this approach (in our view, the currently most consistent) an attempt is made to combine the quantum-mechanical direct process of breakup of the incident ion or stripping of a heavy fragment by the target with a multistep dissipative nature of the interaction of the nuclei. It is assumed that the direct process of transfer of a fragment b from the incident ion $I(=a+b)$ (or its breakup) is accompanied by appreciable dissipation of kinetic energy and angular momentum of the relative motion in the entrance and exit channels:

$$\begin{aligned} I(=a+b)+A &\xrightarrow{\text{diss}} I^*+A^* \\ &\xrightarrow{\text{dir}} a'+B'(=b+A) \\ &\xrightarrow{\text{diss}} a+B(\varepsilon_B^f, L_B^f). \end{aligned} \tag{8}$$

The coupling of the channels of inelastic excitation of the nuclei is modeled by means of phenomenological friction forces (with allowance for the disruption of the channel coherence), and the direct transition process is described by the standard amplitude of the distorted-wave method. The introduction of friction forces into the formalism of quantum collision theory makes it possible to avoid using an imaginary part of the optical potentials of the interaction of the nuclei and, conserving unitarity, to trace the distribution of the incident flux over the intermediate channels.

The use of the semiclassical approximation for the three-dimensional distorted waves and the introduction of so-called transition lines, near which a given process is localized, made it possible to reduce the differential cross section of the multistep (quasidirect) process of formation of light particles a to a readily calculable expression containing an integration over all the intermediate states of the nuclei in the entrance and exit channels. The results obtained by means of this expression demonstrated fairly good agreement with experiment in a wide range of energies and angles of the light particles (see the theoretical curves in Figs. 6, 7, and 13).

The main conclusions obtained in the framework of this approach are the following:

1) The angle and energy distributions of the fast light particles are sensitive to the magnitude of the potential and dissipative internuclear forces at comparatively small distances in the region beyond the Coulomb barrier ($r \leqslant R_C^B$).

2) Weak friction with short range or deep internuclear potentials are in clear disagreement with the experimental data. This means that even nuclei that are not very heavy are, as they penetrate each other, decelerated by dissipative forces rather than accelerated by the potential forces of attraction.

3) Light particles emitted with high energy ($E_a \sim E_a^{\max}$) or at large angles ($\vartheta_{\text{LP}} > \vartheta_{\text{gr}}^{in}$) are produced predominantly in massive-transfer reactions with the maximum (possible for given E_a) prior dissipation of the kinetic energy in the entrance channel. The production of light particles with lower energies (corresponding to the beam velocity) and emitted at small angles occurs mainly when there is incomplete dissipation of the kinetic energy.

4) At initial energies greater than 10 MeV/nucleon, the yield of light particles with velocities $v_a \leqslant v_{\text{beam}}$ at small angles is due to the multistep process of breakup of the incident ion, and the stripping process makes a significant contribution only at large angles and at high E_a.

A shortcoming of the approach is also the serious uncertainty (admittedly less) in the establishment of the absolute values of the differential cross sections.

3.6. Boltzmann equation and "molecular dynamics"[101–116]

In the region of intermediate energies, the dynamics of nucleus–nucleus collisions is often described by means of a Boltzmann equation (also called a Vlasov–Nordheim equation or Boltzmann–Uehling–Uhlenbeck equation) for the single-particle Wigner distribution function $f(r,k,t)$ in phase space:[101–105]

$$\begin{aligned} &\frac{\partial f_1}{\partial t}+\bar{v}\bar{\nabla}_r f_1-\bar{\nabla}_r U\bar{\nabla}_p f_1 \\ &=\frac{4}{(2\pi)^3}\int d^3\bar{k}_2 d^3\bar{k}_3 d\Omega \sigma_{nn}(\Omega) v_{12}[f_3 f_4(1-f_1) \\ &\times(1-f_2)-f_1 f_2(1-f_3)(1-f_4)] \\ &\times\delta^3(\bar{k}_1+\bar{k}_2-\bar{k}_3-\bar{k}_4). \end{aligned} \tag{9}$$

Here, σ_{nn} and v_{12} are the differential cross section and relative velocity of colliding nucleons, $f_i \equiv f(r,k_i,t)$, the single-particle mean field $U(\rho)$ is determined through the equation of state (for example, $U(\rho)=-356(\rho/\rho_0)+303(\rho/\rho_0)^{7/6}$ (MeV)[104]) and is a functional of the energy, and the density $\rho(r)=\int(d^3k/(2\pi)^3)f(r,k,t)$. In actual calculations, an isotropic nucleon–nucleon scattering cross section $4\pi\sigma_{nn}(\Omega)\sim 20$–$40$ mb is usually employed.

By means of the Boltzmann equation one can obtain the mass, velocity, and angular momentum of the residual nuclei as functions of the impact parameter, and also the multiplicity and differential cross section for production of free nucleons. It is much harder (and impossible without additional assumptions) to obtain the yield of light fragments. There are also technical difficulties associated with the integration of (9) over the time, which must be done over a sufficiently long interval to distinguish the bound and unbound nucleons (which are usually distinguished by the value of their potential energy) but not so long that the final nuclei have completely evaporated.

Close in spirit to this approach is the method of so-called molecular dynamics (classical[105–109] and quantum[110–114]), in which either the colliding nuclei are regarded as a collection of classical nucleons interacting through two-body forces and moving in accordance with a system of coupled Newton equations or (in quantum molecular dynamics) each nucleon is described by means of a Gaussian wave packet in phase space:

$$f_1(r,p)=N\exp\left(-\frac{(r-R_i)^2}{\Delta^2}-\frac{(p-P_i)^2}{\hbar^2/\Delta^2}\right). \qquad (10)$$

Here, $R_i(t)$ and $P_i(t)$ are the position and momentum of the wave packet of the ith nucleon, and they are found from the classical equations of Newton with a Hamiltonian that is some functional of the density $\rho_i(r)=\int(d^3p/(2\pi)^3)f_i(r,p)$ that ensures an appropriate binding energy and incompressibility of nuclear matter.

Stochastic two-nucleon collisions are taken into account as follows. If two nucleons approach to a distance $r_{nn}=\sqrt{\sigma_{nn}/\pi}$ ($\sigma_{nn}\sim$20–40 mb is the total nucleon–nucleon cross section), then they are scattered through a randomly chosen angle, allowance being made at the same time for the blocking due to the Pauli principle, which does not allow them to enter already occupied states. The nucleons are usually separated into free and clustered nucleons in this approach in the simplest manner, on the basis of their spatial separation. Since as a result of the time integration the coordinates of all nucleons are known, one can, comparing their mutual separation with a certain fixed $d_{nn}\sim 3$ fm, divide all nucleons into those that are "completely free" and those that belong to certain fragments. The spatial criterion for clustering of nucleons can be strengthened by the additional requirement of proximity in the momentum space: $|p_i-p_k|\leqslant p_F$.

Nevertheless, in this approach there remain problems, which are associated with the stability of the nuclei and clusters and which, in a numerical calculation, require additional "cooling" procedures. In this connection, we must mention the studies of Refs. 115 and 116, in which a similar model is used, not for the nucleons, but directly for α particles, i.e., ^{20}Ne, for example, is regarded as a collection of five α particles that interact with each other and with the target nucleus and move in accordance with the classical equations of Newton.

The main advantages of approaches of this kind is the possibility of considering all nuclear reactions (fragmentation, transfer, fusion) in the framework of one model and the same equations. Each event, specified by an impact parameter and initial orientation of the "molecules" (nucleons or α particles), is calculated separately "to the end," i.e., is decomposed with respect to all the exit channels in which we are interested.

Of course, in such models one can make no claim to a high accuracy in the determination of the differential cross section of some particular process. However, the "conservation of unitarity" (conservation of the total flux and total reaction cross section) is a barrier to systematic errors (lowering or raising of the cross sections of all reactions) and makes it possible to predict not only the relative but also the absolute yields in all channels. Unfortunately, a detailed analysis of the production of light particles in the framework of such approaches has not yet been made.

4. WHAT WE SHOULD LIKE TO KNOW OR CLARIFY

4.1. Relative role of the different mechanisms of production of light particles

For a start, we could distinguish the four groups of processes (mechanisms) of production of light particles in heavy-ion collisions at low and medium energies.

1) The process of complete fusion of the nuclei with subsequent evaporation of light particles a from the compound nucleus or from fission fragments. The characteristic feature of the evaporated particles is their low energy and isotropic distribution. The evaporation spectrum can be calculated fairly accurately, but it is much more difficult to estimate its absolute magnitude (like the total fusion cross section).

2) The two-body primary process of incomplete fusion with emission of only one pre-equilibrium light particle:

$$I+A\to A^*+a(NE)\to\begin{cases}B+\{n,\gamma,p,\alpha\}\\ \cdots\cdots\\ f_1+f_2\\ f_1+f_2+\text{LP.}\end{cases}$$

The light particles a produced in such a process may be fast (up to energies corresponding to the two-body kinematic limit $E_a^{\max}$) or slow (in the presence of strong dissipation of the kinetic energy in the entrance channel). In the latter case, they cannot be distinguished from the evaporated particles. In principle, they could be produced either from projectile nucleons (massive-transfer process) or from target nucleons (substitution process). The characteristic feature of these particles is that they cannot be accompanied by other fast light particles or projectilelike fragments, though they can be accompanied by slow (evaporation) light particles, neutrons, or fission fragments.

3) The two-body primary process of few-nucleon transfer or inelastic excitation ($\Delta N=0$) with subsequent decay of an excited projectilelike nucleus:

$$I+A\to A'(=A\pm\Delta N)+I'(=I\pm\Delta N)\to\begin{cases}a+\text{PLF}+X\\ a_1+a_2+X\end{cases}$$
$$A'(=A\pm\Delta N)\to\begin{cases}B+\{n,\gamma,p,\alpha\}\\ \cdots\cdots\\ f_1+f_2\\ f_1+f_2+\text{LP.}\end{cases}$$

In this process, both fast and slow light particles can be produced. In the first case they will *necessarily* be accompanied by *fast* projectilelike fragments or other fast light particles a_2; in the second case (when the dissipation is high) they will be accompanied by only slow fragments. The nucleons ΔN can be transferred both from the projec-

tile to the target ($m_a+m_{\rm PLF}<m_I$) as well as in the opposite direction ($m_a+m_{\rm PLF}>m_I$). In this group of mechanisms we must also include the processes of deep inelastic excitation of the target and projectile (with their subsequent decay) not accompanied by mass transfer ($\Delta N=0$) or with mutual exchange of equal numbers of nucleons.

4) The quasielastic process of breakup of the incident ion:

$$I+A\to A(E^*\cong 0)+a+b(I-a) \qquad \text{(a)}$$

and the quasielastic process of knockout of a light particle from the target:

$$I+A\to B(=A-a,E^*\cong 0)+a+I. \qquad \text{(b)}$$

It would seem that these processes are the easiest ones to distinguish (in experiments on coincidence of the corresponding particles when $Q_3\cong 0$), but even today we do not know their exact contribution to the total yield of light particles as a function of E_a, ϑ_a, E_I, m_I. As we have already noted, to estimate the total cross section of the three-body process it is necessary to integrate over all angles of the conjugate fragment, and it is very difficult to do this without use of 4π detectors. It was shown above (Sec. 1.5) that process 4 (a) makes up a significant fraction (up to 25% at $E_I\sim 30$ MeV/nucleon) of all breakup processes. With regard to the quasielastic knockout reaction, practically nothing can be said (its cross section may be negligibly small).

Of course, processes 2 and 3 include several possible mechanisms leading to the same final states. However, even with such a crude division, we are not able today with confidence to determine the fraction of each of the four processes in the complete spectrum of light particles as a function of their energy and emission angle and also as a function of the energy and mass of the incident ion.

Figure 36 shows schematically the α-particle spectra at energy $\sim$20 MeV/nucleon for the most forward emission angles and for an angle exceeding the angle of a grazing collision in the entrance channel. The relative contributions of processes 1–4 are indicated by the corresponding curves, which are also very nominal. On the basis of the experience that we currently have, we can put forward the following propositions. The relative contributions of the different processes depend strongly on the energy and mass of the incident ion and on the emission angle of the light particle. At low energies ($\leqslant$10 MeV/nucleon) it seems clear that processes 1 and 2 are dominant, and at higher energies processes 3 and 4. Processes 3 and 4 give greater directionality than process 2, which is dominant at $\vartheta_a+\vartheta_{\rm gr}^{\rm in}$ in the high-energy part of the light-particle spectrum. For light ions ($A_I\leqslant 10$), the role of dissipative processes is weak and a maximum of the yield in reactions 2 and 3 must be observed at energies corresponding to the beam velocity.

Of course, we should wish these propositions to be unambiguously confirmed (or refuted) by the experiments, and Fig. 36 to be no longer schematic but drawn for at least some specific reactions with absolute values of the contributions of the different mechanisms of light-particle production. In such a case, we could also concentrate

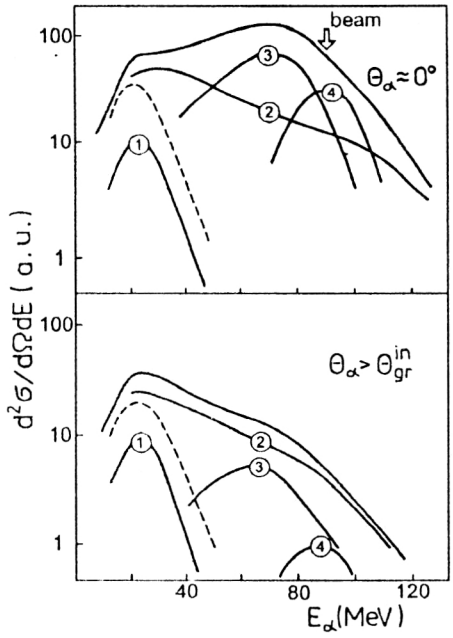

FIG. 36. Schematic representation of the energy spectrum of α particles and of the presumed contributions of the four mechanisms of their production (see the text) at beam energy $\sim$20 MeV/nucleon: 1) evaporation from compound nucleus; 2) incomplete fusion; 3) "inelastic breakup"; 4) elastic breakup (fragmentation). The broken curve is the sum of all evaporated particles (from the compound nucleus and from final nuclei formed in processes 2 and 3).

greater theoretical efforts on the understanding and elucidation of the properties of particular processes identified experimentally. It is possible that experiments using 4π detectors will bring us closer to this goal.

4.2. Two-nucleus interaction dynamics in general and light-particle production processes in particular

The large (but finite) number of particles, the simultaneous manifestation of quantum and classical properties, and the complicated (nonlinear) nature of the interaction of the particles—all this makes the process of interaction of two nuclei at low and medium energies extremely attractive not only from the point of view of problems of nuclear physics but also from the point of view of general theoretical (general physical) problems of understanding nonlinear "stochastic" quantum systems and the appearance of new physical processes, concepts, and theories.

At energies $\geqslant$5 MeV/nucleon, at least half of all the light particles are produced in the earliest initial stage of collision of the two nuclei, before thermodynamic equilibrium is established and the nuclei "forget" their entire prehistory. Thus, by studying the properties and behavior of these particles, we obtain information about this very interesting and least studied stage of the internuclear interaction. We should here like to identify some (in our view, unresolved) problems of the dynamics of two-nucleus interactions, without an understanding of which and without the possibility of more or less accurate description of it one

can hardly hope to give a convincing explanation of the properties of specific nuclear reactions, including processes involving the production of light particles.

Potential forces

The mean field of the nucleus is one of the most fundamental characteristics. However, while the role of the mean field is fairly clear in processes involving the interaction of nucleons with nuclei, in the case of nucleus–nucleus collisions we actually know practically nothing about not only the potential energy of the interaction of the two nuclei but also the potential energy of separation of nucleons (except for the case of nonoverlapping nuclei, when the Coulomb forces are dominant in the internuclear interaction). The presence of potential barriers in the interaction of not too heavy nuclei (due to the superposition of Coulomb and nuclear forces) is not in doubt. However, while we can in some way or other determine the height of these barriers (to within a few mega-electron-volts), we have practically no idea about the shape of the "internal part" of the potential barrier. We are not even able to say with confidence whether two comparatively heavy nuclei are accelerated or decelerated beyond the barrier ($r \leqslant R_c^B$). Down to what distances can we speak of a potential energy of the interaction of two nuclei as they penetrate each other? What is the role of internuclear potential forces in collisions with heavy ions and in the production of light nuclei? There exist different points of view—from complete neglect of the internuclear forces to the assertion that the light particles (or the projectilelike fragments accompanying them) are deflected predominantly to negative angles by these forces.[7,15,117] A large strength of these forces is also invoked to explain the sharp decrease of the transverse flux of light particles in nucleus–nucleus collisions at energies 70–80 MeV/nucleon[118] (scattering through negative angles due to forces of attraction at low energies is replaced by predominant repulsion due to strong contraction at high energies).

It is obvious that it is essential for us to establish the strength of the internuclear potential forces if we wish to achieve a quantitative understanding of the properties of the various reactions. These forces occur in practically all the theoretical models: They determine the field of classical trajectories (in particular, caustic surfaces and focusing of nucleons), the local momenta, distorted waves, barrier penetrabilities, etc. The rapid departure of the nuclei from the elastic channel when they touch makes it impossible to establish the strength of these forces from an analysis of experimental data on elastic scattering (the region beyond the radius of strong absorption is completely invisible). Therefore, it is necessary to seek other reactions whose cross sections are sensitive to the strength of the internuclear potential forces at comparatively short distances. One such reaction is, as it happens, incomplete fusion (massive transfer) with emission of a fast light particle—see in particular Fig. 7a.

Dissipative forces

Internuclear friction forces are no less important in determining the two-nucleus interaction dynamics.[119–133] However, their strength and nature have been established up to now even less well than for the potential forces. It should be noted that dissipative forces are much more informative (and physical) than the imaginary part of the optical potential. They do not simply replace the absorptive part $iW(r)$, determining the reduction of the flux in the elastic channel, but also make it possible to trace the distribution of this flux over the other channels, thereby greatly reducing the uncertainty in the calculation of the absolute values of the various inelastic processes. In our view, it should be the standard practice in heavy-ion physics, whenever possible, to give up the use of an imaginary part of an optical potential and to introduce the more general physical notion of dissipative forces. A possibility has recently appeared for using them not only in classical models but also in the framework of quantum collision theory.[99]

The experimental and theoretical investigations of deep inelastic scattering of heavy ions do not yet permit an unambiguous determination of the strength of the dissipative forces. The parameters of the friction forces (mainly, their strength) deduced by different authors fluctuate in wide ranges. In addition, we are not able to answer the most basic questions relating to dissipative forces. What is the mechanism of energy dissipation—single-particle excitations in a time-dependent mean field, two-nucleon collisions, channel coupling, randomization of the motion of the nucleons in an asymmetric two-center field? If different mechanisms play a part, what is the ratio of their importance as a function of the energy and masses of the colliding nuclei? Is there a certain minimum time needed for energy dissipation, or do there exist mechanisms of "fast" dissipation? Is it in principle possible to separate strictly the potential and dissipative forces in experiments in heavy-ion physics?

Dynamics of the fusion process[126,134,135]

It is assumed that at low energies the fusion channel is dominant in the total cross section of the reaction for the interaction of not too heavy nuclei. For this reason alone it warrants particular attention. However, despite the fact that hundreds of experimental and theoretical studies have been devoted to this problem, we still do not have a complete picture of the dynamics of the process of fusion of two nuclei. What forces the nuclei to maintain their individuality even in the presence of their very strong overlapping in deep inelastic reactions? What keeps the nucleons near their centers and prevents their rapid "collectivization"? Are potential pockets obligatory if the process of fusion is to be possible? What happens with increasing mass of the nuclei: why does the fusion cross section decrease rapidly (by orders of magnitude) at $A_{\text{comp}} \geqslant$??? (Ref. 136)? Why are the mass distributions of the fission fragments of the same nucleus obtained as a result of fusion of different initial pairs of nuclei different (Ref. 137)? What is the

mechanism of below-barrier fusion, and what role is played here by dissipative forces? What is the role of the fission barrier of the compound nucleus? How can one reduce the related processes of fusion and fission (and also radioactivity of heavy ions) to a unified problem in the framework of a general quantum-mechanical model? This list of questions can be continued.

Fragmentation dynamics

The fast process of breakup of the projectile into two (or several) comparatively heavy fragments is quite unlike the fission reaction. What is the mechanism of such a process? Simplified "high-energy" fragmentation models (of the participant–spectator type) have little validity at energies $\leqslant 100$ MeV/nucleon. In "molecular dynamics" (see above) the main attention is devoted to the nucleon degrees of freedom, whereas what is most interesting at low and intermediate energies is the search for and investigation of the collective (coherent) phenomena in heavy-ion collisions such as processes of massive transfer, fast breakup of a heavy projectile, large momentum transfers to a complete nucleus or to heavy clusters without their disintegration, etc.

Instabilities

The presence of nonlinear effects, the departure from spherical symmetry, the dissipative forces, and the quantum nature of the motion of the nucleons make the interaction dynamics of two nuclei not only very complicated but also very interesting from the point of view of the occurrence of all kinds of instabilities. Above all, there is the instability with respect to the transition from regular motion of the nucleons to chaotic motion and the appearance of the associated viscosity of nuclear matter.[132,133] The presence of potential barriers, nuclear forces of attraction, and dissipative forces may lead to the appearance of stable structures different from the initial configuration (self-organization), especially in the case of motion with "large amplitudes," i.e., at above-barrier energies. The high excitation energy introduced into a nucleus leads to an obvious chemical instability with respect to transition of a liquid phase to a gaseous phase. Finally, if the region of negative compression coefficients is entered ($k=\rho(\partial p/\partial\rho)<0$), mechanical instability becomes possible—the nucleus can break up into lighter fragments.[138] At the present time, there has been at best only a qualitative treatment of these phenomena in simplified classical models. Analysis of such effects in realistic quantum approaches (which almost certainly will lead to the discovery of new physical phenomena) is of great interest.

5. POSSIBLE EXPERIMENTS (REQUESTS TO EXPERIMENTALISTS)

The inclusive spectra of light particles should be measured, not at the main peak, but at least within 2–3 orders of magnitude (so that the high-energy tail of the particles can be seen) and for several emission angles (less than, greater, and $\sim\vartheta_{gr}^{in}$). It would be extremely interesting to measure the dissipative part of the spectrum ($v_{LP}<v_{beam}$) at energies $\geqslant 100$ MeV/nucleon at at angles exceeding the angle of a grazing collision.

It is sensible to study *coincidences with characteristic KX radiation* only at low energies of the incident ion. It is desirable to detect in coincidence with the *KX* radiation the broadest possible spectrum of light particles and their angular distributions. It would be very attractive to obtain the absolute values of the double differential cross sections with final nucleus distinguished: $d^2\sigma/d\Omega_{LP}dE_{LP}(Z_{res})$. Our predictions are that for $v_{LP}\sim v_{beam}$ and $\vartheta_{LP}\leqslant\vartheta_{gr}^{in}$ coincidences with $Z_{res}\cong Z_{targ}$ must be dominant, while for $v_{LP}>v_{beam}$ and $\vartheta_{LP}>\vartheta_{gr}^{in}$ coincidences with $Z_{res}\cong Z_{targ}+Z_{proj}-Z_{LP}$ (binary reaction of incomplete fusion) must be.

Coincidences with projectilelike fragments and other light particles should be used to establish the exact contributions of the breakup processes to the yield of light particles. The use of 4π detectors must make it possible to establish, finally, the absolute cross sections of the process of quasielastic breakup of the projectile, $\sigma(4)$, and also the sum $\sigma(3)+\sigma(4)$ (see Sec. 4.1). The most important thing appears to be the separation of the contributions of these processes as functions of the energy and emission angle of the light particle (Fig. 3b). Anticoincidences of light particles with projectilelike fragments or with other fast light particles in 4π experiments will make it possible to separate the massive-transfer channel. However, one must also necessarily have a scenario with respect to the velocities of the detected particles: It is necessary to measure the yield of *fast* light particles with $v_{LP}>v_{beam}$ that are not in coincidence with *fast* projectilelike fragments or other light particles. The initial energies must be such that the light particles with energy corresponding to the velocity of following and with energy corresponding to the Coulomb barrier in the exit channel are well separated. For example, for $V_c^B(\alpha)\cong 20$ MeV and for $E_\alpha(\text{beam})=100$ MeV one can measure the E_α spectrum in the range 50–150 MeV in anticoincidence with other light particles having energy $\geqslant 10$ MeV/nucleon in order to establish the role of the incomplete-fusion channel in this region.

Coincidences with fission fragments may be particularly informative in 4π experiments. Using heavy targets, one can study processes of dissipative breakup: $I+A\rightarrow LP+PLF+f_1+f_2$. Measuring the momenta of the light particle and of the fission fragments and selecting events with $(p_{LP}^{\parallel}+p_{f_1f_2}^{\parallel})/P_{beam}\cong 1$, one can easily separate the contribution of the binary process of incomplete fusion. This process can also be separated by measuring $LP+f_1+f_2$ in anticoincidence with another fast light particle or projectilelike fragment. In this case, the main interest is also in obtaining the dependence of such events on the energy and emission angle of the light particle. Measurement of the charges of fission fragments with $Z_1+Z_2>Z_{targ}$ will make it possible to establish unambiguously the transfer processes, the very existence of which at high energies ($\geqslant 100$ MeV/nucleon) is in doubt. For this purpose, one can measure once more events corresponding to processes of complete or incomplete fusion in the

$\vartheta_{f_1 f_2}$ distributions (see Fig. 30), choosing as targets readily fissioning nuclei and lighter projectiles.

Coincidences with γ rays can be used above all to separate the angular momenta and to convert the cross section to the form $d\sigma/db$, in which it depends on the impact parameter in the entrance channel. Optimal experiments in this respect are those using "triple" coincidences ("channel $+M_\gamma$"), which make it possible to estimate the values of the impact parameters that make the main contribution to the investigated reaction channel: LP+PLF+M_γ with the use of $d\sigma_{\text{breakup}}/db$, or LP−PLF+$M_\gamma$ with the use of $d\sigma_{\text{stripping}}/db$, etc. It would be interesting, for example, to consider the possibility of an incomplete-fusion reaction with emission of a *fast* light particle, not in a peripheral collision, but in a central one—coincidences LP+$KX(Z_{\text{res}})$+M_γ with $Z_{\text{res}}=Z_{\text{targ}}+Z_{\text{proj}}-Z_{\text{LP}}$ and $M_\gamma \cong 0$. Such events would correspond to a process of "shake-off" of external nucleons from the projectile and their coherent focusing in the field of the nucleus.[139]

One further possibility for converting the differential cross sections to a dependence on the impact parameter is the method of "global variables,"[140,141] used in experiments with 4π detectors. The essence of the method is to detect as far as possible all products of a particular event. One then determines "global characteristics" of the event such as the multiplicity ν of the light particles, their total charge $\Sigma_i^\nu z_i$, the total transverse momentum $\Sigma_i^\nu m_i v_i \sin\vartheta_i$, and the mean longitudinal velocity $v_{\text{av}}=(\Sigma_i^\nu m_i v_i \cos\vartheta_i)/\Sigma_i^\nu m_i$. The most unambiguous correspondence is found between the impact parameter in the entrance channel and the mean parallel velocity ($v_{\text{av}} \cong v_{\text{CN}}$ for $b=0$ and $v_{\text{av}} \cong v_{\text{beam}}$ for $b \cong R_1+R_2$). Thus, by sorting the events in accordance with the values of the mean longitudinal velocity v_{av}, they can be approximately sorted according to the values of the impact parameters (instead of using vague definitions of "central" and "peripheral" collisions).

We note, in conclusion, that analysis of each individual event detected in 4π experiments will undoubtedly make it possible to obtain much more information than in "traditional" experiments. However, the best method of analyzing these events (with the aim of extracting the maximum amount of sufficiently reliable information) is yet to be developed.

[1] H. C. Britt and A. R. Quinton, Phys. Rev. **124**, 877 (1961).
[2] H. Homeyer *et al.*, Phys. Rev. C **26**, 1335 (1982).
[3] Ch. Egelhaaf *et al.*, Nucl. Phys. **A405**, 397 (1983).
[4] H. Homeyer *et al.*, Z. Phys. A **314**, 143 (1983).
[5] H. Fuchs *et al.*, Phys. Rev. C **31**, 465 (1985).
[6] M. Bürgel *et al.*, Phys. Rev. C **36**, 90 (1987).
[7] W. Terlau *et al.*, Z. Phys. A **330**, 303 (1988).
[8] J. Uckert *et al.*, Phys. Lett. **206B**, 190 (1988).
[9] J. Van Driel *et al.*, Phys. Lett. **98B**, 351 (1981).
[10] J. Wilczynski *et al.*, Nucl. Phys. **A373**, 109 (1982).
[11] R. K. Bhowmik *et al.*, Nucl. Phys. **A390**, 117 (1982).
[12] R. H. Siemssen *et al.*, Phys. Lett. **161B**, 261 (1985).
[13] G. J. Balster *et al.*, Nucl. Phys. **A468**, 93 (1987).
[14] G. J. Balster *et al.*, Nucl. Phys. **A468**, 131 (1987).
[15] G. J. Balster *et al.*, Nucl. Phys. **A471**, 635 (1987).
[16] B. Kotlinski *et al.*, Nucl. Phys. **A526**, 303 (1991).
[17] E. Gierlik *et al.*, E7-12922, JINR, Dubna (1979).
[18] C. Borcea *et al.*, E7-80-363, JINR, Dubna (1980).
[19] C. Borcea *et al.*, Nucl. Phys. **A391**, 520 (1982).
[20] C. Borcea *et al.*, Nucl. Phys. **A415**, 169 (1984).
[21] V. V. Kamanin *et al.*, Nucl. Phys. **A431**, 545 (1984).
[22] A. V. Belozerov *et al.*, R7-88-388 [in Russian], JINR, Dubna (1988).
[23] W. Augustyniak *et al.*, Z. Phys. A **332**, 209 (1989).
[24] T. Fukuda *et al.*, Nucl. Phys. **A425**, 548 (1984).
[25] G. D. Westfall *et al.*, Phys. Lett. **116B**, 118 (1981); D. K. Scott, Nucl. Phys. **A409**, 291 (1983).
[26] Z. Chen *et al.*, Nucl. Phys. **A473**, 564 (1987).
[27] F. Deak *et al.*, Phys. Rev. C **42**, 1029 (1991).
[28] J. A. Pinston *et al.*, Phys. Lett. **167B**, 375 (1986).
[29] T. Inamura *et al.*, Phys. Lett. **68B**, 51 (1977).
[30] L. Westerberg *et al.*, Phys. Rev. C **18**, 796 (1978).
[31] D. R. Zolnowski *et al.*, Phys. Rev. Lett. **41**, 92 (1978).
[32] K. Siwek-Witczynska *et al.*, Nucl. Phys. **A330**, 150 (1979).
[33] K. A. Geoffroy *et al.*, Phys. Rev. Lett. **43**, 1303 (1979).
[34] J. H. Barker *et al.*, Phys. Rev. Lett. **45**, 424 (1980).
[35] C. M. Castaneda *et al.*, Phys. Rev. C **21**, 179 (1980).
[36] R. L. Robinson *et al.*, Phys. Rev. C **24**, 2084 (1981).
[37] H. Yamada *et al.*, Phys. Rev. C **24**, 2565 (1981).
[38] H. Tricoire *et al.*, Z. Phys. A **306**, 127 (1982).
[39] H. Utsunomia *et al.*, Phys. Rev. C **28**, 1975 (1983).
[40] C. Gerschel *et al.*, Z. Phys. A **322**, 433 (1985).
[41] T. Inamura *et al.*, Phys. Rev. C **32**, 1539 (1985).
[42] H. Tricoire *et al.*, Z. Phys. A **323**, 163 (1986).
[43] M. N. Namboodiri *et al.*, Phys. Rev. C **35**, 149 (1987).
[44] R. Billerey *et al.*, Z. Phys. A **292**, 293 (1979).
[45] H. Ho *et al.*, Phys. Lett. **96B**, 51 (1980).
[46] E. Takada *et al.*, Phys. Rev. C **23**, 772 (1981).
[47] W. D. M. Rae *et al.*, Phys. Lett. **105B**, 417 (1981).
[48] E. Takada *et al.*, Phys. Lett. **118B**, 307 (1982).
[49] T. Fukuda *et al.*, Phys. Rev. C **26**, 2029 (1983).
[50] P. L. Gonthier *et al.*, Nucl. Phys. **A411**, 289 (1983).
[51] H. Ho *et al.*, Phys. Rev. C **27**, 584 (1983).
[52] M. Sasagase *et al.*, Phys. Rev. C **27**, 2630 (1983).
[53] P. B. Goldhorn *et al.*, Phys. Lett. **142B**, 14 (1984).
[54] W. D. M. Rae *et al.*, Phys. Rev. C **30**, 158 (1984).
[55] A. C. Shotter *et al.*, Phys. Rev. Lett. **53**, 1539 (1984).
[56] T. Shimoda *et al.*, J. Phys. Soc. Jpn. **55**, 3031 (1986).
[57] G. Bizard *et al.*, Phys. Lett. **172B**, 301 (1986).
[58] R. Vandenbosch *et al.*, Phys. Rev. C **37**, 998 (1988).
[59] S. B. Gazes *et al.*, Phys. Lett. **208B**, 194 (1988).
[60] M. Stern *et al.*, Z. Phys. A **331**, 323 (1988).
[61] P. L. Gonthier *et al.*, Phys. Rev. C **41**, 2635 (1990).
[62] J. Pouliot *et al.*, Phys. Rev. C **43**, 735 (1991).
[63] J. Pouliot *et al.*, Phys. Lett. **263B**, 18 (1991).
[64] P. J. Siemens *et al.*, Phys. Lett. **36B**, 24 (1971).
[65] A. N. Bice *et al.*, Nucl. Phys. **A390**, 161 (1982).
[66] J. Pochodzalla *et al.*, Phys. Lett. **174B**, 36 (1986).
[67] T. C. Awes *et al.*, Phys. Lett. **87B**, 43 (1979).
[68] V. E. Viola *et al.*, Phys. Rev. C **26**, 178 (1982).
[69] L. Schad *et al.*, Z. Phys. A **318**, 179 (1984).
[70] E. Duck *et al.*, Z. Phys. A **317**, 83 (1984).
[71] G. Bizard *et al.*, Nucl. Phys. **A456**, 173 (1986).
[72] H. Fatyga *et al.*, Phys. Rev. C **35**, 568 (1987).
[73] K. A. Griffioen *et al.*, Phys. Rev. C **37**, 2502 (1988).
[74] R. Lacey *et al.*, Phys. Rev. C **37**, 2540 (1988).
[75] D. Jacquet *et al.*, Nucl. Phys. **A511**, 195 (1990).
[76] D. J. Parker *et al.*, C **30**, 143 (1984).
[77] A. Budzanowski *et al.*, Phys. Rev. C **32**, 1534 (1985).
[78] J. Pochodzalla *et al.*, Phys. Lett. **181B**, 33 (1986).
[79] D. J. Parker *et al.*, Phys. Rev. C **35**, 161 (1987).
[80] A. Malki *et al.*, Z. Phys. A **339**, 283 (1991).
[81] A. Chbini *et al.*, Phys. Rev. C **43**, 652 (1991).
[82] E. C. Pollacco *et al.*, Phys. Lett. **146B**, 29 (1984).
[83] V. E. Bunakov and V. I. Zagrebaev, Z. Phys. A **333**, 57 (1989).
[84] D. K. Srivastava, D. N. Basu, and H. Rebel, Phys. Lett. **206B**, 391 (1988).
[85] F. Rami *et al.*, Z. Phys. A **327**, 207 (1987).
[86] K. A. Frankel and J. D. Stevenson, Phys. Rev. C **23**, 1511 (1981).
[87] D. Guerreau, Nucl. Phys. **A447**, 37c (1985).
[88] A. S. Goldhaber, Phys. Lett. **53B**, 306 (1974).
[89] W. A. Friedman, Phys. Rev. C **27**, 569 (1983).
[90] T. C. Awes *et al.*, Phys. Rev. C **24**, 89 (1981).
[91] F. Rami *et al.*, Nucl. Phys. **A444**, 325 (1985).

[92] V. E. Bunakov, V. I. Zagrebaev, and A. A. Kolozhvari, Izv. Akad. Nauk SSSR **52**, 1311 (1980).
[93] T. Udagawa and T. Tamura, Phys. Rev. Lett. **45**, 1311 (1980).
[94] V. E. Bunakov and V. I. Zagrebaev, Z. Phys. A **304**, 231 (1982).
[95] V. I. Zagrebaev and A. Yu. Kozhin, Izv. Akad. Nauk SSSR **52**, 104 (1988).
[96] E. Takada *et al.*, Phys. Rev. C **23**, 772 (1981).
[97] T. Udagawa, D. Price, and T. Tamura, Phys. Lett. **116B**, 311 (1982).
[98] V. I. Zagrebaev, Yad. Fiz. **44**, 80 (1986) [Sov. J. Nucl. Phys. **44**, 51 (1986)].
[99] V. I. Zagrebaev, Ann. Phys. (N.Y.) **197**, 33 (1990).
[100] V. I. Zagrebaev, *Nuclear Reactions (Proc. of the First Kiev Intern. School on Nuclear Physics)* (Kiev, 1990), p. 471.
[101] G. F. Bertsch *et al.*, Phys. Rev. C **29**, 673 (1984).
[102] J. Aichelin and G. F. Bertsch, Phys. Rev. C **31**, 1730 (1985).
[103] G. F. Bertsch and S. Das Gupta, Phys. Rep. **160**, 189 (1988).
[104] M. B. Tsang *et al.*, Phys. Rev. C **40**, 1685 (1989).
[105] L. Wilets *et al.*, Nucl. Phys. **A282**, 341 (1977).
[106] A. R. Bodmer, C. N. Panos, and A. D. MacKellor, Phys. Rev. C **22**, 1025 (1980).
[107] R. J. Lenk and V. R. Pandharipande, Phys. Rev. C **34**, 177 (1986).
[108] T. J. Schlagel and V. R. Pandharipande, Phys. Rev. C **36**, 162 (1987).
[109] R. J. Lenk, T. J. Schlagel, and V. R. Pandharipande, Phys. Rev. C **42**, 372 (1990).
[110] J. Aichelin *et al.*, Phys. Rev. C **37**, 2451 (1988).
[111] G. Peilert *et al.*, Phys. Rev. C **39**, 1402 (1989).
[112] D. M. Boal and J. N. Glosli, Phys. Rev. C **38**, 1870, 2621 (1988).
[113] H. Feldmeier, Nucl. Phys. **A515**, 147 (1990).
[114] T. Maruyama, A. Ohnishi, and H. Horiuchi, Phys. Rev. C **42**, 386 (1990).
[115] R. Mohring, T. Srokowski, D. H. E. Gross, and H. Homeyer, Phys. Lett. **203B**, 210 (1988).
[116] A. Szczurek *et al.*, Z. Phys. A **338**, 187 (1991).
[117] M. B. Tsang *et al.*, Phys. Rev. Lett. **57**, 559 (1986).
[118] J. P. Sullivan *et al.*, LPC Caen, Report LPCC 90-04 (1990).
[119] R. Beck and D. H. E. Gross, Phys. Lett. **47B**, 143 (1973).
[120] D. H. E. Gross, Nucl. Phys. **A240**, 472 (1975).
[121] J. P. Bondorf *et al.*, Phys. Rev. C **11**, 1265 (1975).
[122] H. H. Deubler and K. Dietrich, Phys. Lett. **56B**, 241 (1975).
[123] K. Albrecht and W. Stocker, Nucl. Phys. **A278**, 95 (1977).
[124] J. Randrup, Ann. Phys. (N.Y.) **112**, 356 (1978).
[125] J. Blocki *et al.*, Ann. Phys. (N.Y.) **113**, 330 (1978).
[126] P. Fröbrich, Phys. Rep. **116**, 337 (1984).
[127] A. Van Geertruyden and Ch. Leclercq-Willain, Nucl. Phys. **A459**, 173 (1986).
[128] J. L. Neto, Ann. Phys. (N.Y.) **173**, 443 (1987).
[129] M. Münchow and W. Scheid, Nucl. Phys. **A468**, 59 (1987).
[130] S. Pal and D. H. E. Gross, Z. Phys. A **329**, 349 (1988).
[131] P. Fröbrich and S. Y. Xu, Nucl. Phys. **A477**, 143 (1988).
[132] W. J. Swiatecki, Nucl. Phys. **A488**, 375c (1988).
[133] W. J. Swiatecki, Report LBL-29482, Berkeley (1990).
[134] U. Mosel, *Treatise on Heavy Ion Science*, edited by D. A. Bromley, Vol. 2 (New York, 1984), p. 3.
[135] G. R. Satchler, M. A. Nagarajan, and J. S. Lilley, Ann. Phys. (N.Y.) **178**, 110 (1987).
[136] A. N. Andreev *et al.*, in *International Seminar School on Heavy Ion Physics*, D7-90-142 [in Russian] (JINR, Dubna, 1990), p. 499; A. B. Quint, Report GSI-89-22, Dissertation, TH Darmstadt.
[137] P. Gippner *et al.*, Z. Phys. A **325**, 335 (1986).
[138] D. K. Scott, Nucl. Phys. **A409**, 291 (1983).
[139] V. I. Zagrebaev, JINR Int. School on Nucl. Phys., Kiev (1991).
[140] J. Peter *et al.*, Phys. Lett. **237B**, 187 (1990).
[141] J. Peter *et al.*, LPC Caen, Report LPCC 90-03 (1990).

Translated by Julian B. Barbour